International Immunopharmacology 172 (2026) 116223

Contents lists available at ScienceDirect

International Immunopharmacology

journal homepage: www.elsevier.com/locate/intimp

Neuronal pentraxin 2 in peripheral sensory neurons drives chronic itch through potentiation of the interleukin-31/interleukin-31 receptor pathway in atopic dermatitis

Xue-Qiang Bai [a,b,1], Bing-Xin Wu [a,1], Ji-An Wang [c,1], Cheng He [a], Yong-Liang Shen [d], Xiao Wei [a], Yu-Qi Zhang [a], Xue-Wen Chen [c], Rong Sun [a], Qun-Feng Gui [d], Juan Wang [a], Zhi-Jun Zhang [a,e,*]

[a] Department of Human Anatomy, Medical School of Nantong University, Nantong, Jiangsu 226001, China
[b] Department of Basic Medical Science, Jiangsu Medical College, Yancheng, Jiangsu 224005, China
[c] Department of Dermatologic Surgery, Shanghai Skin Disease Hospital, Tongji University, Shanghai 200443, China
[d] Department of Neurosurgery, the Sixth Affiliated Hospital of Nantong University, Yancheng Third People's Hospital, Yancheng, Jiangsu 224008, China
[e] Jiangsu Province Key Laboratory in University for Inflammation and Molecular Drug Target, Nantong University, Nantong, Jiangsu 226001, China

ARTICLE INFO

Editor Name: Dr. Yongchun Shen

Keywords:
Pruritus
NPTX2
Interleukin-31
Trigeminal ganglion
Atopic dermatitis

ABSTRACT

Atopic dermatitis (AD) is one of the most prevalent chronic inflammatory skin conditions, primarily characterized by intense itching that leads to scratching and presents a challenging clinical issue with incompletely understood mechanisms. Neuronal pentraxin 2 (NPTX2) is associated with neurodevelopment, synaptic plasticity, and neuroinflammation in the central nervous system. In this study, we aimed to thoroughly investigate the peripheral role of NPTX2 in mediating chronic itch in AD. Real-time polymerase chain reaction (PCR), immunohistochemistry, ELISA assays, western blot, and small interfering RNA (siRNA) intervention were performed to explore the peripheral role of NPTX2 in an AD model. We demonstrated that NPTX2 was selectively upregulated in small- and medium-sized trigeminal ganglion (TG) neurons in the MC903-induced AD model, and was transported to peripheral nerve terminals. Importantly, protein expression of NPTX2 was significantly elevated in the skin nerves of patients with AD. Notably, NPTX2 administration alone, intradermally, provoked moderate scratching behavior in mice. However, *Nptx2* and neuronal pentraxin receptor (NPTXR) siRNA intra-TG injection significantly attenuated scratching behaviors in AD mice. Critically, NPTXR, its cognate receptor, was specifically localized to pruriceptive calcitonin gene–related peptide-positive neurons ($CGRP^{+}$) and isolectin B4 ($IB4^{+}$) neuronal subsets. Mechanistically, NPTX2 synergizes with interleukin-31 (IL-31), a well-known pruritic cytokine in AD, to potentiate phosphorylated-extracellular signal-regulated kinase (p-ERK) signaling in primary sensory neurons. PD98059, the inhibitor of p-ERK, significantly alleviated the scratching induced by the combination of NPTX2 and IL-31. Additionally, PD98059 also significantly reduced the upregulation and release of NPTX2 caused by IL-31 stimulation. Our results offer a new understanding of the molecular mechanisms underlying chronic pruritus in the MC903-induced AD model, highlighting NPTX2-dependent signaling as a key therapeutic strategy for refractory itch disorders.

1. Introduction

Atopic dermatitis (AD) is a prevalent and recurrent inflammatory skin condition characterized by a complex interplay of multiple underlying factors. Studies have shown that approximately 20% of children and 10% of adults are affected by AD [1]. The key clinical symptoms of AD include pruritus (itching), rashes, and dry skin. Pruritus initiates a vicious itch-scratch cycle, in which scratching damages the epidermal barrier and facilitates the penetration of environmental allergens (*e.g.*, house dust mites) [2,3]. This breach promotes a type 2 inflammatory response, characterized by cytokines such as interleukin (IL)-4, IL-13, and IL-31, primarily secreted by T helper 2 cells, which further sensitize sensory nerve fibers and exacerbate itching [4]. This creates a self-perpetuating cycle of itch–scratch–itch, making the condition

* Corresponding author at: Department of Human Anatomy, Medical School of Nantong University, Nantong, Jiangsu 226001, China.
E-mail address: zhzhj@ntu.edu.cn (Z.-J. Zhang).
[1] These authors contributed equally to this work.

https://doi.org/10.1016/j.intimp.2026.116223
Received 20 August 2025; Received in revised form 21 December 2025; Accepted 13 January 2026
Available online 20 January 2026

particularly difficult to manage and significantly affecting the patient's quality of life [4]. Management of AD can also exacerbate social and familial costs [5]. Despite its prevalence, there is limited basic and clinical research on AD and a lack of effective antipruritic therapies [6]. Therefore, the development of new therapeutic targets and anti-itch drugs for AD is urgently needed.

Pentraxins are a family of phylogenetically conserved molecules characterized by a cyclic multimeric structure [7], which are expressed in multiple tissues and regulate innate immune and inflammatory responses [8]. Neuronal pentraxin 2 (NPTX2), a member of the pentraxin family, is a secreted immediate early gene product [9]. Direct interaction of NPTX2 with the neuronal pentraxin receptor (NPTXR) is involved in the removal of synaptic debris [10]. Changes in NPTX2 expression have been observed in a variety of diseases, including Alzheimer's disease [11,12], cutaneous squamous cell carcinoma [13], epithelial ovarian cancer [14], and colorectal carcinoma [15]. Elevated NPTX2 also promotes dorsal hippocampal synaptic remodeling and accelerates the extinction of cocaine-related contextual memory [16]. In addition, previous studies have demonstrated that NPTX2 knockdown does not affect inflammatory pain, neuropathic pain, and acute pain-related behaviors [17]. Considering the involvement of NPTX2 in immune activity and inflammatory responses that orchestrate the pathological progression of atopic dermatitis, we hypothesize that NPTX2 plays a previously unrecognized role in AD-associated chronic itch. Notably, NPTX2 expression (both gene and protein) displayed a dose-dependent elevation 6 h after lipopolysaccharide administration [18]. This newly identified pro-inflammatory cytokine, NPTX2, outperforms existing immunological biomarkers in predicting Alzheimer's disease-related outcomes, highlighting its potential importance in immunoregulation [19].

IL-31, discovered in 2004 by Dillon et al. [20], belongs to the glycoprotein 130 /IL-6 cytokine family and is characterized by a four-helix bundle structure. IL-31 can be produced by activated T cells, especially T helper type 2 cells [21]. The IL-31 receptor complex comprises two subunits: IL-31 receptor alpha (IL-31RA) and oncostatin M receptor (OSMR), which together form a functional heterodimer [22]. Notably, IL-31RA specifically contributes to the formation of the IL-31 receptor, whereas OSMR exhibits functional versatility by partnering with glycoprotein 130 to form the OSMR complex [22]. IL-31 is a pivotal pruritogenic cytokine in AD [23]. IL-31RA is expressed on immune cells, keratinocytes, and neurons [24–26], and is overexpressed in peripheral nerve fibers and dorsal root ganglia in AD models [27,28]. Thus, the IL-31/IL-31RA axis is critically important in chronic pruritus [29]. The binding of IL-31 to its receptor triggers an inflammatory cascade *via* janus-activated kinase/signal transducer and activator of transcription, phosphatidylinositol 3-kinase, and extracellular signal-regulated kinase (ERK) pathways [30]. Persistent ERK phosphorylation (p-ERK) has been observed in sensory neurons of mice with chronic itching [31]. P-ERK is a unique marker of spinal itch signaling and represents an attractive target for the treatment of chronic itch [32,33].

Here, we chose the MC903-induced AD model, which is consistent with many of the key transcriptional changes observed in human chronic itch [34] and is considered an ideal model for studying chronic pruritus. We found that NPTX2 expression was elevated and predominantly localized in small-and medium-diameter neurons in AD mice. Under the condition of persistent itching, NPTX2 was trafficked to the peripheral nerve terminals in the skin. A single subcutaneous injection of recombinant NPTX2 induced only mild scratching; however, NPTX2 potentiated IL-31–induced dramatic scratching, and NPTX2 small interfering RNA (siRNA) knockdown attenuated MC903-induced pruritic behaviors.

2. Materials and methods

2.1. Animals

Adult male and female C57BL/6 wild-type mice (8 weeks old) were obtained from the Experimental Animal Center of Nantong University. Mice were housed under conditions approved by the Nantong Committee on Animal Care and Use, including a 12-h light/dark cycle (lights on from 07:00 to 19:00), a temperature of 22 °C (± 2 °C), and 60% humidity. Animals were provided with standard rodent chow and water *ad libitum* in a controlled environment. Mice were randomly assigned to either experimental or control groups for behavioral testing. The exact number of animals (n) in each experimental group is explicitly stated in the respective figure legends for all *in vivo* experiments. All behavioral experiments were conducted by investigators blinded to group allocation and treatment (approval number: IACUC20211215–1001).

2.2. Chronic AD model and acute itch model

Mice were acclimatized for 3 days after being purchased from the Nantong University Laboratory Animal Center. Following anesthesia with isoflurane, facial hair was removed using an epilator, and depilatory cream was applied to the depilated areas for 3 min. Upon completion of hair removal, mice were returned to their housing cages and continued feeding for an additional 3 days. To induce chronic AD lesions, the mice were treated with MC903 (CAS: 112965–21-6, #HY-10001, MCE, NJ, USA) on the cheeks, following previously described methods [34]. In brief, MC903 (20 μL at a concentration of 200 μM) was applied to the cheek once daily for 10 consecutive days. The control group received the same treatment, with vehicle (absolute ethanol) applied instead of MC903.

For the acute itch model, pruritogens, including compound 48/80 (CAS: 848035–21–2, #C2313, Sigma-Aldrich, MO, USA), histamine (HIS) (CAS: 51–45-6, #59964, Sigma-Aldrich), IL-31 (#51070-M08H, SinoBiological, Beijing, China), and NPTX2 (#19880-H02H, SinoBiological), were intradermally injected into the facial area. Scratching behavior was quantified by blinded observers using video recording (iPhone 12 Pro Max) for 1 h post-injection.

2.3. Behavior test

Mice were individually placed in plastic boxes for 30 min to acclimate to the new environment, and this process was repeated for three consecutive days. In the acute itch model, scratching behavior was recorded for 1 h after intradermal injection of pruritogens. For the MC903-induced chronic itch model, scratching behavior was recorded for 1 h following each application of MC903. Scratching behavior was quantified as follows: when a mouse used its hind paw to scratch the facial injection site or nearby areas, then licked or bit its paw, or placed the paw back onto the floor, this entire sequence was counted as one scratching event. To ensure objective assessment, all experimental procedures were conducted under blinded conditions.

2.4. Real-time quantitative polymerase chain reaction (qPCR)

Total RNA from trigeminal ganglion (TG) tissue was extracted using Trizol reagent (#15596026, Invitrogen, CA, USA). One microgram of RNA was reverse transcribed using a reverse transcription kit (#AG11728, Accurate Biology, Changsha, China), following the manufacturer's instructions. qPCR analysis was performed using a real-time detection system with SYBR Green (#AG11740, Accurate Biology). The amplification cycling conditions were as follows: Step 1, 95 °C for 30 s; Step 2, 95 °C for 5 s, 60 °C for 30 s, for 40 cycles. Primers were purchased from Sangon Biotech, China. The following primers were used: GAPDH: forward 5′-TGT TCC TAC CCC CAA TGT G-3′, reverse 5′-GTG TAG CCC AAG ATG CCC T-3′; NPTX2: forward 5′-ACG GGC AAG

GAC ACT ATG G-3′, and reverse 5′-ATT GGA CAC GTT TGC TCT GAG-3′. qPCR reactions were run on a StepOnePlus™ system (Life Technologies, Gaithersburg, MD, USA). Target gene expression was quantified using the $2^{-\Delta\Delta CT}$ method, with GAPDH messenger RNA (mRNA) as the reference gene for normalization.

2.5. Hematoxylin and eosin (HE) staining

Skin tissue specimens were collected on day 10 following MC903 application and were immediately fixed in 4% neutral buffered formalin. After fixation, the tissues were dehydrated through a graded ethanol series (70%, 80%, 95%, and 100%), cleared in xylene, and subsequently embedded in paraffin wax. Serial sections of 5 μm thickness were prepared using a rotary microtome. The sections were then rehydrated and stained with HE. Stained sections were examined under a microscope, and epidermal thickness was quantified using ImageJ software, with the mean value of the control group serving as the reference for normalization.

2.6. Molecular docking

Models of NPTXR and the IL-31 receptor were constructed by homology modeling using the AlphaFold3 online tool (https://alphafoldserver.com/). First, the UniProt IDs of NPTXR, IL-31RA, and OSMR were identified and submitted to AlphaFold3 to obtain the top 10 predicted structures (models 0–9). The results were then ranked based on the predicted accuracy of protein–protein interactions, and the top five models (models 0–4) were retained for further analysis.

2.7. Primary culture of TG neurons

Following isoflurane-induced anesthesia, mice were euthanized by cervical dislocation. The TGs were carefully dissected and placed in ice-cold Hank's Balanced Salt Solution (#C0219, Beyotime, Shanghai, China), followed by three washes to remove blood from the surface. The ganglia were then enzymatically dissociated using collagenase (CAS: 9001-12-1, #C9891, Sigma-Aldrich) and dispase-II (CAS: 42613–33-2, #D4693, Sigma-Aldrich), in a 37 °C water bath for 35 min. After enzyme digestion, the tissue was further treated with 0.25% trypsin-ethylenediaminetetraacetic acid (#25200056, Gibco, NY, USA) for 5 min. To eliminate tissue debris and cell clusters, the suspension was passed through a 70 μm cell strainer. The cells were then resuspended in Neurobasal™-A medium (#A2477501, Gibco) supplemented with penicillin-streptomycin (#SV30010, Cytiva, MA, USA), GlutaMAX (#35050061, Gibco), and B27 supplement (#17504044, Gibco) and plated onto 6-well plates or culture dishes pre-coated with poly-D-lysine (#A3890401, Gibco). Plates were incubated overnight at 37 °C in a 5% CO_2 incubator. The cultured neurons were then used for subsequent experiments.

2.8. Western blot

Cells or tissues were homogenized in radio-immunoprecipitation assay buffer (#P0013B, Beyotime) containing 1 mM phenylmethylsulfonyl fluoride (#ST506, Beyotime), 1 mM phosphatase inhibitors (#P1005, Beyotime), and protease inhibitors (#4906837001, Roche, Basel, Switzerland), and incubated on ice for 30 min. The lysates were then centrifuged at 12,000 rpm for 20 min at 4 °C to collect the supernatant. Protein concentration was determined using a bicinchoninic acid protein assay kit (#P0010, Beyotime). Based on the protein concentration, the volume was adjusted to load 30 μg of protein per lane. Proteins were separated by 10% SDS-PAGE (#E303–01, Vazyme, Nanjing, China) and transferred to a polyvinylidene difluoride membrane. The polyvinylidene difluoride membrane was blocked with 5% non-fat dry milk (#P0216, Beyotime) or 5% bovine serum albumin (#ST023, Beyotime) at room temperature for 2 h, followed by overnight incubation at 4 °C with primary antibodies: NPTX2 (rabbit, 1:200, #10889–1-AP, Proteintech, Wuhan, China), p-ERK (rabbit, 1:1000, #4370 T, CST, MA, USA), ERK (rabbit, 1:1000, #4695 T, CST), NPTXR (rabbit, 1:400, #anr-193-50ul, Thermo Fisher Scientific, MA, USA), IL-31RA (rabbit, 1:1000, #PA5–76851, Thermo Fisher Scientific), OSMR (rabbit, 1:1000, #84888–2-RR, Proteintech), and GAPDH (mouse, 1:20000, #60004–1-Ig, Proteintech).

The following day, membranes were washed three times and incubated with the secondary antibodies: horseradish peroxidase-conjugated goat anti-rabbit immunoglobulin G (IgG) (1:10000, #SA00001–2, Proteintech) or horseradish peroxidase-conjugated goat anti-mouse IgG (1:10000, #SA00001–1, Proteintech) at room temperature for 2 h. After washing three times, protein bands were visualized using enhanced chemiluminescence (#E411–04, Vazyme). Band intensities were quantified using ImageJ software and normalized to ERK and GAPDH.

2.9. Coimmunoprecipitation (co-IP)

Co-IP was performed using a commercial kit (#Cat. KTD104, Abbkine Scientific, Wuhan, China) to investigate the potential interaction between NPRXR and IL-31RA/OSMR. Briefly, mouse skin tissue was homogenized on ice for 5 min, followed by centrifugation at 13,400 ×*g* for 10 min at 4 °C to remove debris. Protein concentration was quantified at 1 μg/μL using a bicinchoninic acid assay.

For immunoprecipitation, protein A/G beads (20 μL) were washed three times and resuspended in a 1.5 mL tube. Washed beads were incubated with 1.5 μL anti-NPTXR antibody or 2 μL rabbit IgG (control) for 30 min at room temperature. Antibody-bound beads were then incubated with the protein supernatant overnight at 4 °C. The immunoprecipitated samples were collected for subsequent western blot analysis.

2.10. ELISA assay

The ELISA kits for mouse NPTX2 (#YT-47806 M1, Nanjing, China) and IL-31 (#YT-45495 M1, Nanjing, China) were purchased from Jiangsu Yutong Biotechnology Company. ELISA was performed on cell culture supernatants following the manufacturer's instructions. For each assay, 25 μL of supernatant was used. Blank, standard, and sample wells were set up for each experiment. NPTX2 and IL-31 levels were quantified by zeroing the instrument with blank wells and measuring absorbance at 450 nm.

2.11. Immunohistochemistry

Each mouse was anesthetized with isoflurane, and cardiac perfusion was performed with 20 mL of 0.9% saline, followed by 50 mL of ice-cold 4% paraformaldehyde. The TG and facial skin were subsequently harvested. The TG and skin tissues were post-fixed overnight at 4 °C and underwent sucrose gradient dehydration using 20% and 30% sucrose solutions (#ST1670, Beyotime) at 4 °C. The tissues were then sectioned into 14-μm slices using a cryostat.

For immunohistochemistry, sections were incubated overnight at 4 °C with the following primary antibodies: NPTX2 (rabbit, 1:200, #10889–1-AP, Proteintech), NPTXR (rabbit, 1:200, #anr-193-50ul, Thermo Fisher Scientific), CGRP (mouse, 1:2000, #C7113, Sigma-Aldrich), NF200 (mouse, 1:1000, #MAB5266, Millipore, MA, USA), glial fibrillary acidic protein (mouse, 1:1000, #MAB360, Millipore), Tuj1 (mouse, 1:1000, #MAB1195, R&D systems, MN, USA), and CD68 (mouse, 1:1000, #Ab955, Sigma-Aldrich). After primary antibody incubation, sections were washed and incubated with the following secondary antibodies at room temperature for 2 h: Alexa Fluor 488-conjugated donkey anti-rabbit IgG (1:1000, #711–545-152, Jackson ImmunoResearch, PA, USA), Cy3-conjugated donkey anti-mouse IgG (1:1000, #715–165-150, Jackson ImmunoResearch), Cy3-conjugated donkey anti-rabbit IgG (1:1000, #711–165-152, Jackson

ImmunoResearch), and IB4-fluorescein isothiocyanate (mouse, 1:1000, #L2895, Sigma-Aldrich).

Following secondary antibody incubation, sections were washed again, incubated with DAPI for 10 min, and mounted with mounting medium before placing coverslips on slides. Fluorescent images were captured using a Zeiss microscope and an Olympus confocal microscope. Quantification of immunofluorescence images for NPTX2 and p-ERK was performed using ImageJ software.

2.12. HEK293 cell culture

HEK293 cells were purchased from the Shanghai Institutes for Biological Sciences, Chinese Academy of Sciences. Cells were cultured in high-glucose Dulbecco's modified Eagle medium (#BC-M-005, Bio-Channel, Nanjing, China) supplemented with 10% fetal bovine serum (#A5256701, Gibco) and 1% penicillin-streptomycin, with experiments conducted after two passages.

The *Nptx2* plasmid (500 ng), siRNAs (500 ng), and negative control (NC) siRNA (OBiO, Shanghai, China) were transfected using Lipofectamine 2000 reagent (#11668500, Invitrogen) for 24 or 48 h. Sequences of the three pairs of *Nptx2* siRNAs were as follows: *Nptx2 Mus-380* 5′-GCU CCU UGC AAA CCC UCA ATT-3′, 5′-UUG AGG GUU UGC AAG GAG CTT-3′; *Nptx2 Mus-707* 5′-GCA AGA UCA AGA AGA CAU UTT-3′, 5′-AAU GUC UUC UUG AUC UUG CTT-3,′ and *Nptx2 Mus-1209* 5′-GGU GGA CAA CAA UGU CGA UTT-3′, 5′-AUC GAC AUU GUU GUC CAC CTT-3′. Sequences of the three pairs of *Nptxr* siRNAs were as follows: *Nptxr Mus-628* 5′-CAA GAU GGA CGA ACU AGA ATT-3′, 5′-UUC UAG UUC GUC CAU CUU GTT-3′; *Nptxr Mus-1002* CAA UGG AGC UGC UGA UCA ATT-3′, 5-UUG AUC AGC AGC UCC AUU GTT-3′; *Nptxr Mus-1251* 5′-GUG ACA UUG CAC AGU UCA ATT-3′, 5-UUG AAC UGU GCA AUG UCA CTT-3′. After transfection, HEK293 cells were harvested for qPCR or western blot analysis to assess the efficiency of RNA interference.

2.13. Drugs and administration

Nptx2 and *Nptxr* siRNA were designed and synthesized by OBiO (Shanghai, China). One optical density unit of siRNA was reconstituted in 125 μL of diethyl pyrocarbonate-treated water and gently mixed by pipette to ensure homogeneity before use. Using a 30 G needle, the siRNA solution was slowly administered to the medial region of the TG *via* the infraorbital foramen toward the foramen rotundum [35,36].

2.14. Patient sample analysis

All human skin biopsies were conducted at Shanghai Dermatology Hospital (Shanghai, China). Samples were collected from both non-lesional and AD-lesional skin of AD patients. The sample collection process was approved by the Ethics Committee of Shanghai Dermatology Hospital (IRB: SSDH-IEC-SG-029-4.2). Written informed consent was obtained from all participants prior to the procedure. Frozen sections of human skin samples were prepared with a thickness of 14 μm, and subsequent analyses were performed using ELISA and immunofluorescence, as previously described in the literature [37].

2.15. Statistical analysis

All statistical analyses were conducted using GraphPad Prism 9.0 (GraphPad). Data are presented as mean ± standard error of the mean. For comparisons between two groups, an unpaired Student's *t*-test was used. For comparisons involving more than two groups, one-way or two-way analysis of variance followed by Bonferroni's *post hoc* test was applied. A p-value <0.05 was considered statistically significant.

3. Results

3.1. Mouse AD model induced by MC903 is characterized by chronic itch, weight loss, increasing facial skin thickening, and weight gain at the lesion site

To induce AD in the mouse cheek, the low-calcemic vitamin D analog MC903 was applied topically to the facial skin as previously described [34] (Fig. 1A). After depilation and acclimatization, mice received once-daily MC903 application to the cheek region for 10 consecutive days. Pruritic behavior was quantified by analyzing 1-h video recordings to count hind-paw scratching bouts throughout the induction period. In male mice, MC903 elicited a sustained increase in scratching behavior beginning on day 5 compared with ethanol vehicle controls (Fig. 1B). Female mice exhibited similar pruritic responses (Fig. 1F), and direct comparison revealed no significant sex-dependent differences in itch intensity or temporal progression.

To assess systemic physiological impacts, we monitored body weight longitudinally in MC903-treated cohorts. Quantitative analysis showed a significant and progressive loss of body weight starting on day 5 after treatment and continuing throughout the 10-day observation period (Fig. 1C and G). This metabolic perturbation paralleled the established pruritic timeline, suggesting potential neuroendocrine-immune axis involvement in MC903-mediated pathophysiology. Comparative analysis of sex-based physiological responses revealed no statistically significant disparities in body weight trajectories between male and female cohorts. We also measured facial skin thickness and skin weight in male and female mice [38]. MC903-treated animals showed similar cutaneous pathology, with significantly increased facial skin thickness and skin weight compared to the vehicle (Fig. 1D-E and H-K). Together, the MC903 mouse model is characterized by chronic itch, weight loss, increasing facial skin thickening, and increased weight at the lesion site.

3.2. NPTX2 is increased in small- and medium-sized TG neurons of AD mice

After successful establishment of chronic AD, we performed RNA-sequencing of the TG tissue from MC903-treated 10-day mice (Fig. 2A). Differential gene expression analysis in RNA-sequencing requires conducting thousands of independent statistical tests across the transcriptome, thereby inflating the false discovery rate. To mitigate this inherent multiple testing burden, we applied rigorous statistical correction methods (*e.g.*, the Benjamini–Hochberg procedure) to control the false discovery rate at a predefined threshold ($\alpha < 0.05$) during hypothesis testing. Accordingly, we identified 76 up-regulated genes and 68 down-regulated genes in MC903 10-day samples (Fig. S1). *Nptx2* was identified as one of the most upregulated genes in the AD model (Fig. 2B and C), and previous studies have also reported the upregulation of NPTX2 in AD mice [34]. Therefore, we chose NPTX2 for follow-up studies. First, we assayed *Nptx2* mRNA expression in TG using qPCR. *Nptx2* mRNA was significantly increased at days 3, 6, and 10 in MC903-treated mice compared to the vehicle group (Fig. 2D).

Immunofluorescence and ELISA demonstrated that NPTX2 protein was low within the TG in the vehicle group but was significantly increased in the MC903 group (Fig. 2E-H).

Given the functional specialization of distinct neuronal subpopulations in sensory processing, we performed dual immunofluorescence labeling to identify the specific neuronal subtypes expressing NPTX2 and to assess its potential role in synaptic plasticity or circuit modulation. Double immunostaining revealed that NPTX2 showed minimal colocalized with macrophage marker (CD68) or the satellite glial cell marker glial fibrillary acidic protein (GFAP) (Fig. 3A and B). In contrast, NPTX2 exhibited strong colocalization with the peptidergic neuronal marker calcitonin gene-related peptide (CGRP), moderate colocalization with the nonpeptidergic neuronal marker isolectin B4 (IB4), and limited colocalization with the large-diameter neuronal

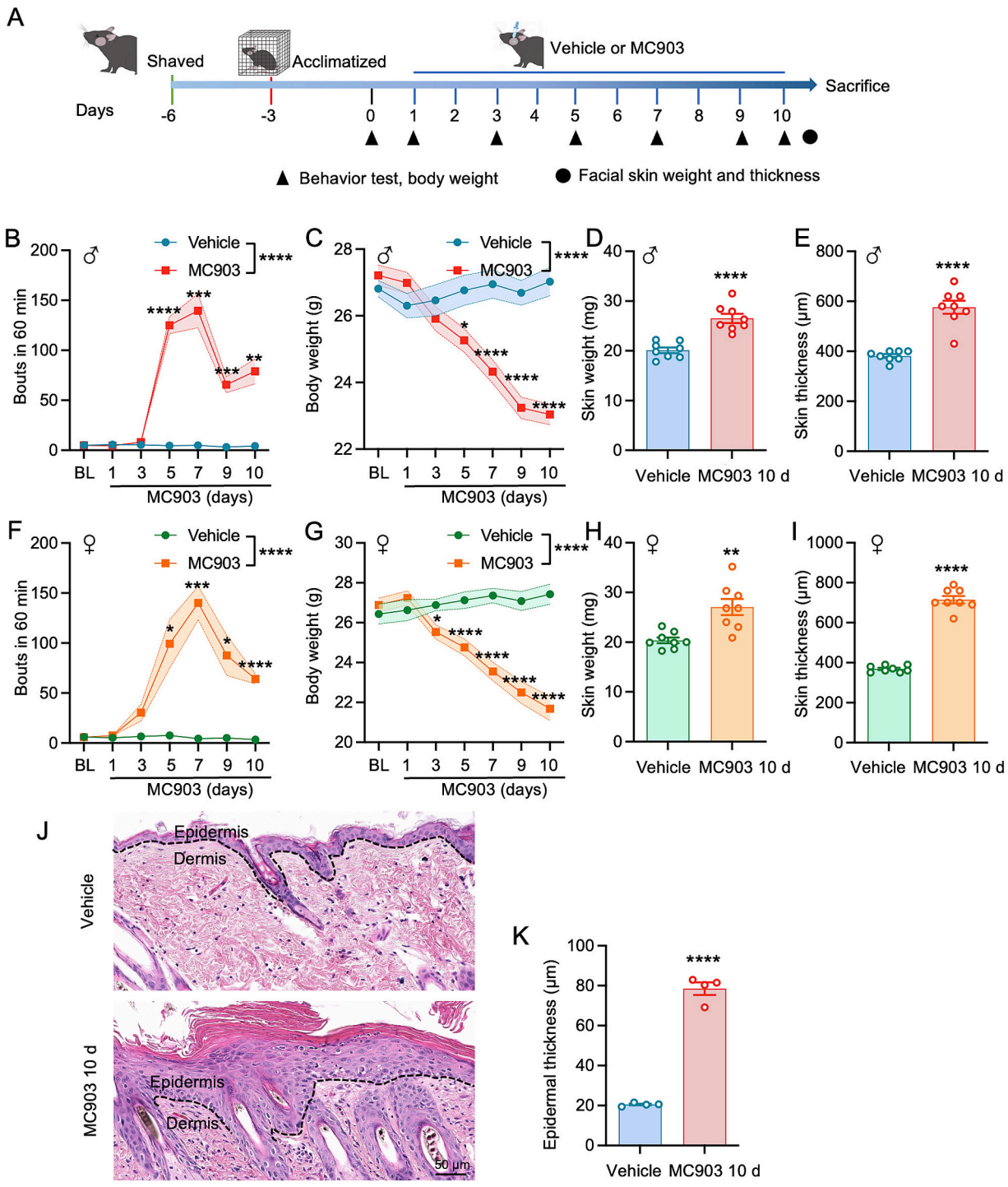

Fig. 1. The Mouse MC903 model is characterized by chronic itch, weight loss, and increased facial skin thickening and weight at the application site. (A) Flowchart of mouse MC903 model. (B) Number of scratches in male mice treated with MC903. ***$P < 0.001$ and ****$P < 0.0001$, compared to male vehicle group. Two-way ANOVA followed by Bonferroni's tests. $n = 8$ mice per group. (C) Changes in body weight of male mice. ***$P < 0.001$ and ****P < 0.0001, compared to male vehicle group. Two-way ANOVA followed by Bonferroni's tests. n = 8 mice per group. (D, E) Facial skin thickness and weight in male mice at day 10 of MC903 and vehicle group. ****$P < 0.0001$, compared to male vehicle group. Student's *t*-test. n = 8 mice per group. (F) Number of scratches in female mice treated with MC903. *$P < 0.05$, **$P < 0.01$ and ****P < 0.0001, compared to vehicle group. Two-way ANOVA followed by Bonferroni's tests. n = 8 mice per group. (G) Changes in body weight of mice in female mice groups. *$P < 0.05$ and ****P < 0.0001, compared to vehicle group. Two-way ANOVA followed by Bonferroni's tests. n = 8 mice per group. (H, I) Facial skin thickness and weight in female mice at day 10 of MC903 and vehicle group. **P < 0.01 and ****P < 0.0001, compared to female vehicle group. Student's *t*-test. n = 8 mice per group. (J) Representative images of HE staining in skin of MC903 10 d mice. Scale bar = 50 μm. Dashed line indicates the border between the epidermis and dermis. (K) Statistical chart of the images in (J). ****P < 0.0001, compared to vehicle group. Student's *t*-test. $n = 4$ mice per group. Data are presented as means ± SEM.

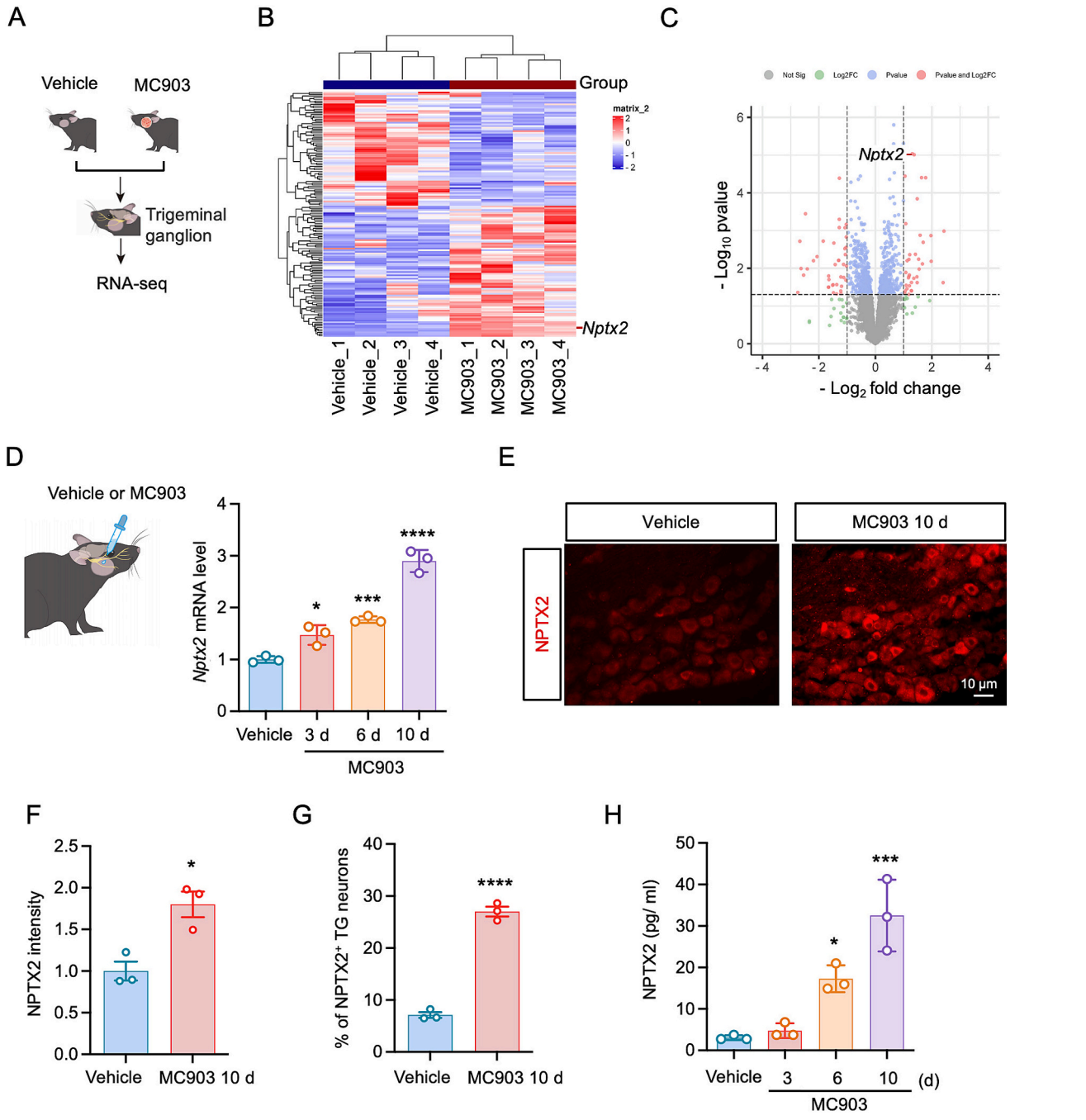

Fig. 2. NPTX2 is upregulated in the TG of the MC903-induced AD model.
(A) Flowchart of RNA-seq analysis. (B, C) Heat maps and volcano plots showing elevated NPTX2 expression in the TG of MC903 10-day mice. (D) The expression of *Nptx2* mRNA in TG at 3, 6, 10 days in MC903 mice. *$P < 0.05$, ***P < 0.001, ****P < 0.0001, compared to vehicle group. Statistical analysis was performed using One-way ANOVA. $n = 3$ mice per group. (E) Immunofluorescence staining showing NPTX2 expression in the TG of vehicle and MC903 10 d mice. Scale bar = 10 μm. (F) Quantification of NPTX2 fluorescence intensity in (E). *$P < 0.05$, compared to vehicle group. Student's *t*-test. n = 3 mice per group. (G) Percentage of $NPTX2^+$ neurons in the TG of vehicle and MC903 10 d mice. ****P < 0.0001, compared to vehicle group. Student's t-test. n = 3 mice per group. (H) NPTX2 levels measured by ELISA in the TG at 3, 6, 10 days in MC903 mice. *P < 0.05, ***P < 0.001, compared to vehicle group. One-way ANOVA by Bonferroni's tests. $n = 3$ mice per group. Data are presented as means ± SEM.

marker NF200 (Fig. 3C-E).

We next characterized the expression pattern of its receptor, NPTXR, in TG neurons from MC903-treated mice at day 10. Immunostaining demonstrated that NPTXR was likewise predominantly expressed in CGRP-positive and IB4-positive neurons, with only limited expression in NF200-positive neurons (Fig. S2).

Collectively, these findings indicate that NPTX2 is upregulated at both the mRNA and protein levels and is primarily localized to small- and medium-diameter TG neurons in the AD mouse model.

3.3. *NPTX2 exacerbates the existing itch*

To assess whether NPTX2 is sufficient to induce itch, we subcutaneously injected recombinant NPTX2 into the mouse cheek and recorded behavioral responses at multiple time points (Fig. 4A). NPTX2 elicited only mild and transient scratching behavior (Fig. 4B). This led us to

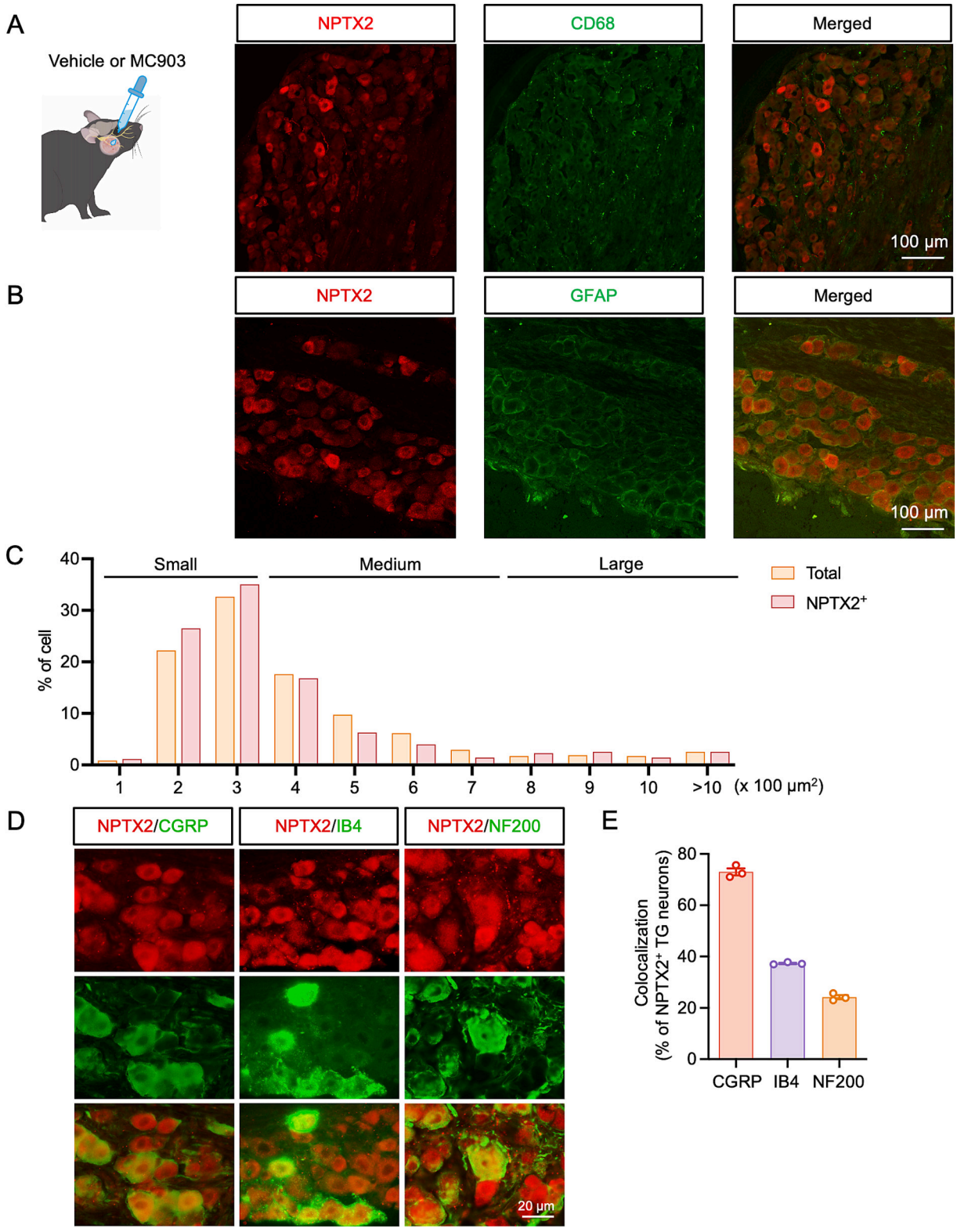

Fig. 3. NPTX2 is distributed in small- and medium-sized neurons.
(A) Representative images of double staining of NPTX2 with CD68 in TG of MC903 10 d mice. Scale bar = 100 μm. (B) Representative images of staining of NPTX2 with GFAP in TG of MC903 10 d mice. Scale bar = 100 μm. (C) Cell size profiling of $NPTX2^{+}$ and total neurons in TG neurons of MC903 10 d mice. (D) Representative images of double staining of NPTX2 with CGRP, IB4, and NF200 in TG of MC903 10 d mice. Scale bar = 20 μm. (E) Statistical chart of the images in (D).

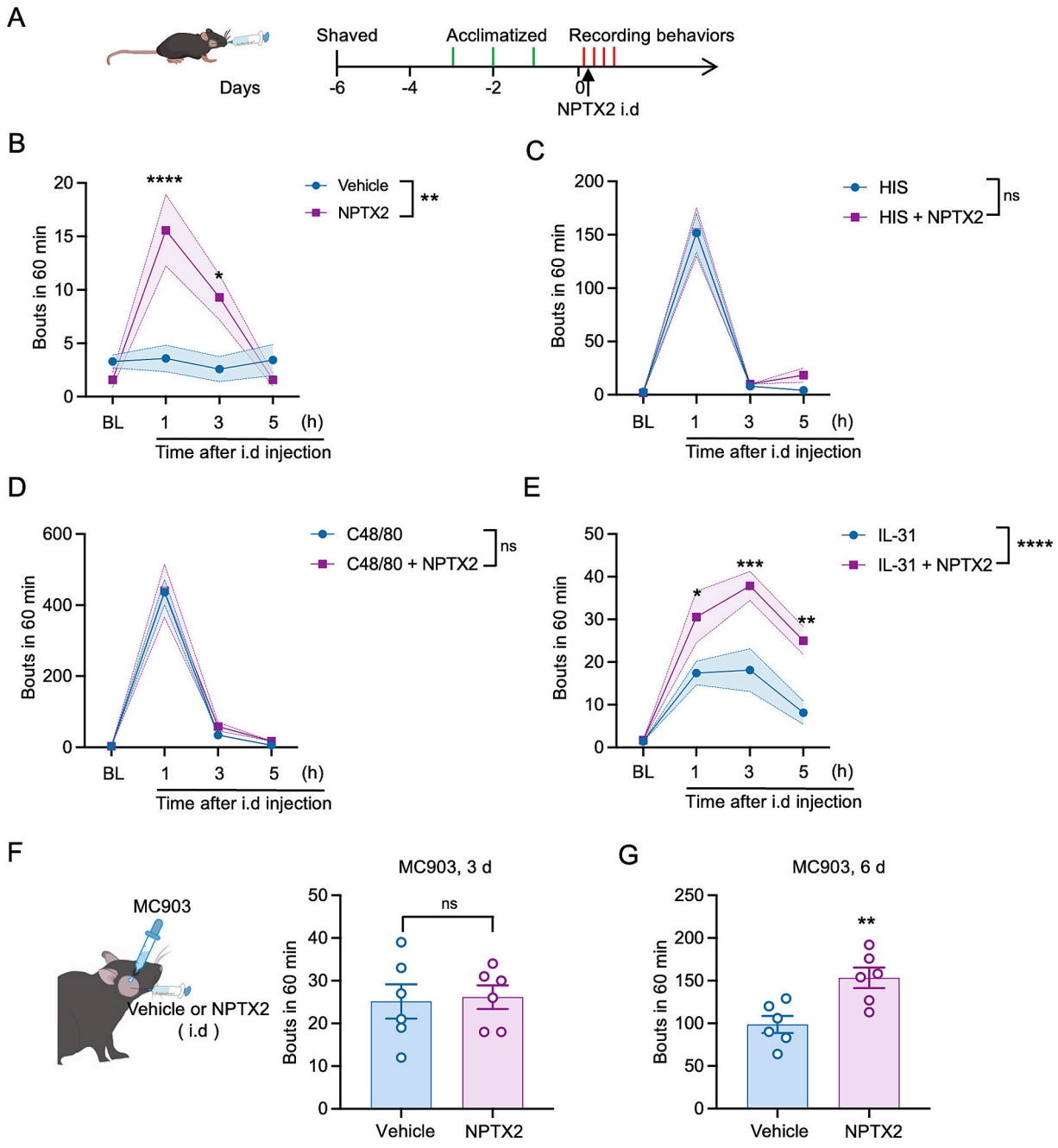

Fig. 4. NPTX2 exacerbates the existing itch.
(A) Graphical representation of the experimental design. (B) Scratching behavior induced by subcutaneous injection of recombinant NPTX2 in cheek. *P < 0.05, **P < 0.01, ****P < 0.0001, compared to vehicle group. Two-way ANOVA followed by Bonferroni's tests. $n = 7$ mice per group. (C and D) Number of scratching bouts after subcutaneous injection of HIS (C) and C48/80 (D) or in combination with NPTX2 into the cheek skin. ns, not significant. Two-way ANOVA followed by Bonferroni's tests. n = 7 mice per group. (E) Scratching behavior following subcutaneous injection IL-31 alone or in combination with NPTX2 in cheek skin. *P < 0.05, **P < 0.01, ***P < 0.001, ****P < 0.0001, compared to the IL-31 alone group. Two-way ANOVA followed by Bonferroni's tests. n = 7 mice per group. (F, G) Scratching numbers of mice treated with subcutaneous injection vehicle or NPTX2 after 3-day (F) and 6-day (G) MC903 application. **P < 0.01, compared to vehicle group. Student's *t*-test. $n = 6$ mice per group. ns, not significant. Data are presented as means ± SEM.

hypothesize that NPTX2 may act synergistically with other pruritogens to amplify itch signaling.

We focused on IL-31, a cytokine strongly implicated in AD pathogenesis [39–41], and on canonical pruritogens associated with acute itch, such as histamine (HIS) [42,43] and compound 48/80 (C48/80) [44]. To evaluate the potential enhancing effect of NPTX2, we administered low doses of each pruritogen mixed with NPTX2. IL-31 is a type 2 inflammation–associated cytokine, while HIS and C48/80 are HIS-dependent pruritogens [44] that independently induce intense itch [44,45]. However, whether additional factors can potentiate IL-31-, HIS-, or C48/80-evoked pruritus has not been previously established [22,46]. Subsequently, the impact of NPTX2 in conjunction with a low dose of pruritogen on acute itch behavior was evaluated. We used a lower dose regimen than previously reported for HIS and C48/80 to assess the effect of NPTX2 in potentiating acute pruritogens [47]. Interestingly, NPTX2 did not enhance HIS- or C48/40-induced scratching responses (Fig. 4C and D). Previous studies have demonstrated that subcutaneous injections of IL-31 at approximately microgram doses or

higher induce significant scratching behavior in mice [48]. Our results revealed that the scratching behavior in the group receiving a mixture of NPTX2 (100 ng) and IL-31 (300 ng) was significantly greater than that observed in the group treated with IL-31 alone. Furthermore, this increased scratching response persisted for more than 5 h (Fig. 4E).

To determine whether NPTX2 accelerates the progression of MC903-induced AD, we administered NPTX2 into the cheek of AD mice at both day 3 and day 6 after MC903 treatment. NPTX2 had no observable effect on scratching during the early stages of AD (Fig. 4F). However, it exacerbated scratching in AD mice at day 6 of MC903 treatment (Fig. 4G). These findings indicate that while NPTX2 induces only mild scratching independently, it can enhance scratching triggered by IL-31, significantly increasing MC903-induced scratching in the late stage.

To further characterize the role of NPTX2 in AD mice, we first screened three pairs of siRNAs targeting *Nptx2* and *Nptxr* for knockdown efficacy in HEK293 cells (Fig. 5A). qPCR measurements confirmed that the *Nptx2* and *Nptxr*-expressing plasmid significantly increased the respective mRNA levels in HEK293 cells compared to the NC group (Fig. 5B and S3A). Among the tested siRNAs, both *Nptx2* and *Nptxr* siRNAs effectively reduced the elevated mRNA levels in plasmid-treated cells (Fig. 5C and S3B). To further evaluate the impact of *Nptx2* siRNAs on NPTX2 protein expression, we conducted a western blot. Results showed that both *Nptx2* Mus-380 and *Nptx2* Mus-707 significantly reduced NPTX2 protein levels compared to the NC group, with the *Nptx2* Mus-707 group exhibiting the lowest protein levels (Fig. S4). Based on these findings, we selected *Nptx2 Mus-707* and *Nptxr Mus-1002* for further *in vivo* studies. Additionally, we modified *Nptx2 Mus-707*, *Nptxr Mus-1002,* and NC siRNA with 2′-methoxy (2'-OMe) and cholesterol to enhance transfection efficiency *in vivo*.

We then examined the number of scratches after intra-TG injection of *Nptx2* and *Nptxr* siRNA in MC903-induced AD mice at day 5 (Fig. 5D). Behavioral data indicated that both *Nptx2* and *Nptxr* siRNA (5 μg) [49] partially reduced MC903-induced scratching bouts from days 1 to 4 post-injection compared to the *NC* siRNA group (Fig. 5E). In contrast, neither *Nptx2* nor *Nptxr* siRNA alleviated MC903-induced weight loss (Fig. 5F). The weight and thickness of the facial skin were significantly decreased in the siRNA-treated mice compared to the NC group (Fig. 5G and H). To confirm the knockdown efficiency of *Nptx2* and *Nptxr* siRNA *in vivo*, we measured the level of *Nptx2* and *Nptxr* mRNA 4 days post-injection. Both *Nptx2* and *Nptxr* siRNA led to a significant reduction in their respective target mRNAs compared to the *NC* group (Fig. 5I). Finally, we demonstrated that intra-TG injection of *Nptxr* siRNA significantly suppressed the scratching behavior induced by the co-administration of NPTX2 and IL-31 (Fig. 5J).

3.4. Neuronal mechanisms of itch involved in NPTX2 combined with IL-31

Following our observation that low doses of IL-31 in conjunction with NPTX2 are sufficient to induce significant scratching behavior, we subsequently explored the underlying mechanisms involved. IL-31-induced itch requires ERK signaling but not phosphorylation of p38 [24]. We collected mouse TGs as shown in Fig. 6A and performed primary neuron cultures. The cultured TG neurons were treated with vehicle, IL-31, NPTX2, and a combination of IL-31 and NPTX2 for 30 min, respectively. We then assessed the levels of p-ERK across the different treatment groups. The western blot results showed that co-incubation of IL-31 with NPTX2 significantly increased the expression of p-ERK compared to either stimulus alone or the vehicle control (Fig. 6B). The western blot results were also verified by immunofluorescence staining of p-ERK in cultured TG neurons (Fig. 6C). Furthermore, intraperitoneal injection of PD98059 (10 μg) [50–54], an inhibitor of ERK activation, significantly attenuated NPTX2-synergistically-enhanced IL-31-induced scratches (Fig. 6D) and reduced p-ERK levels in the TG tissues (Fig. 6E).

Receptor crosstalk confers new signaling and pharmacological properties on neurons, enhancing the ability of neural circuits to regulate diverse behavioral outputs [55]. To determine whether these two receptors physically interact with each other, we built a protein-protein docking model. A predicted TM-score < 0.5 and an interface predicted TM-score < 0.6 indicated that effective interactions are less likely to occur. The docking model showed that NPTXR and the two IL-31 receptors had low interaction scores (Tables 1 and 2) and a low likelihood of interaction (Fig. 7A and B). Subsequently, we performed Co-IP experiments to verify the results from the docking model. We demonstrated that no interaction exists between NPTXR and IL-31RA/OSMR (Fig. 7C). These results indicate that NPTX2 promotes scratching by enhancing IL-31-induced p-ERK signaling, but that NPTXR is less likely to directly interact with IL-31RA and OSMR.

3.5. NPTX2 is synthesized in TG neurons under itchy conditions

It is unknown whether pruritogen stimulation drives the expression and release of NPTX2 from TG neurons. To investigate the effect of pruritic stimuli on TG neurons, we exposed them to IL-31 (33.1 nM) for 6 h. The qPCR results revealed a significant increase in *Nptx2* mRNA levels in TG neurons (Fig. 8A). Given that it takes time for *Nptx2* mRNA to be translated and processed into an active protein that is subsequently released from the cell, we extended the stimulation period to 24 h. We then used an ELISA kit to measure the level of NPTX2 in the cell supernatant. Our findings showed that NPTX2 protein was significantly upregulated at 33.1 nM IL-31 exposure, whereas no significant induction was detected at 6.6 nM (Fig. 8B). This suggests that pruritic stimulation promotes the production and secretion of NPTX2 in TG neurons. Moreover, PD98059 significantly attenuated IL-31-induced *Nptx2* mRNA expression in TG neurons (Fig. 8C). These findings suggest that IL-31 may enhance *Nptx2* gene transcription *via* the ERK signaling pathway. We then sought to confirm whether neuronally-derived NPTX2 is trafficked to peripheral nerve endings *in vivo*. In the skin of MC903-treated mice, ELISA revealed a significant increase in NPTX2 protein (Fig. 8D), whereas qPCR results indicated that *Nptx2* mRNA was not changed in the skin of MC903 10-day mice (Fig. S5). ELISA results also showed that, compared with the vehicle group, IL-31 expression in the skin of MC903-treated mice was significantly elevated on days 6 and 10 (Fig. 8E). We used the neuronal marker Tuj1 to label nerve fibers and found substantial colocalization of NTPX2 and Tuj1 in the skin of AD mice (Fig. 8F). These results demonstrate that TG neurons undergo NPTX2 synthesis with subsequent anterograde axonal trafficking to cutaneous sensory terminals and release it following pruritogenic challenge.

Finally, we examined the NPTX2 level in the skin of AD patients. The ELISA assay demonstrated a significantly elevated expression of NPTX2 in AD-lesional skin compared to non-lesional skin (Fig. 9A). The skin is composed of three layers: the epidermis, dermis, and hypodermis (Fig. 9B). We used skin samples from AD patients for immunofluorescence staining of NPTX2 and Tuj1. The epidermal-dermal junctions were photographed using a fluorescence microscope. Double staining revealed an increased colocalization of NTPX2 and Tuj1 in the skin of AD patients (Fig. 9C).

4. Discussion

AD, a prevalent chronic inflammatory skin disorder, is characterized by chronic pruritus, one of its most debilitating clinical features. Chronic pruritus, a hallmark of inflammatory skin diseases and systemic disorders, remains mechanistically elusive despite its profound clinical burden. This study identifies NPTX2 as a critical amplifier of itch signaling *via* peripheral pathways. Our findings delineate a novel axis in which NPTX2 potentiates pruritogen-induced scratching through ERK/mitogen-activated protein kinase activation and anterograde trafficking to cutaneous nerve terminals, thereby bridging neuronal hyperactivity with the clinical manifestations of chronic itch in AD

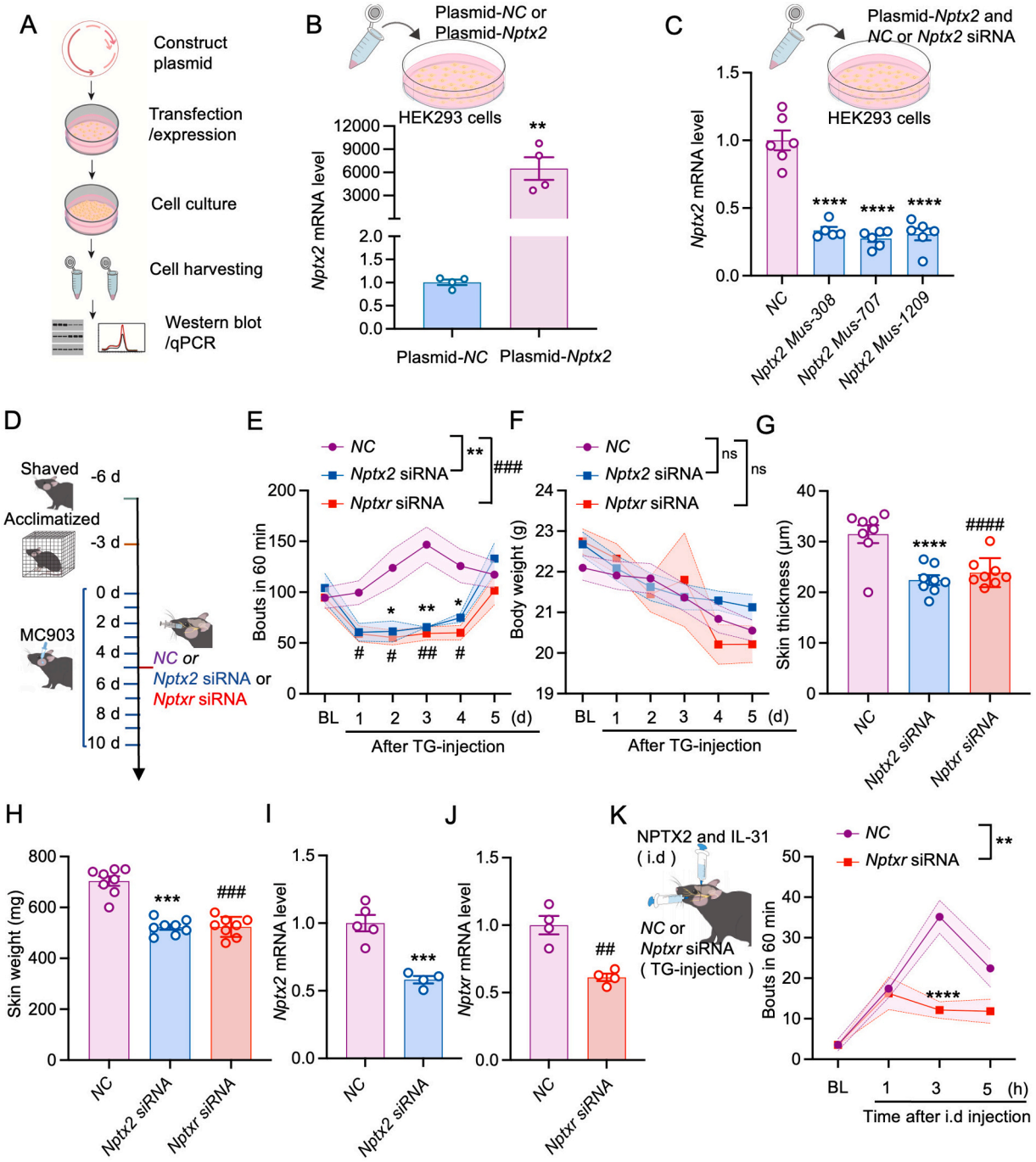

Fig. 5. Inhibition of NPTX2 expression attenuates MC903-induced itching.
(A) Flowchart for the construction of *Nptx2* plasmid and NPTX2 overexpression. (B) qPCR showing *Nptx2* mRNA expression at 6 h after transfection of the plasmid in HEK293 cell line. **P < 0.01, compared to plasmid-*NC* group. Student's test. $n = 4$ mice per group. (C) Down-regulation of *Nptx2* mRNA by treatment with three pairs of *Nptx2* siRNAs in HEK293 cell line. ****P < 0.0001, compared to NC group, One-way ANOVA followed by Bonferroni's tests. $n = 5$ to 6 mice per group. (D) Schematic of the experimental timeline showing intra-TG injection of *Nptx2* and *Nptxr* siRNA, followed by behavioral assays. (*E*-H) MC903-induced scratching (E), weight change (F), facial skin thickness (G) and facial skin weight (H) in mice following intra-TG injection of *Nptx2* and *Nptxr* siRNA (5 μg) or *NC* siRNA. *P < 0.05, **P < 0.01, ***P < 0.001, and ****P < 0.0001, *Nptx2* siRNA *vs NC* group. #P < 0.05, ##P < 0.01, ###P < 0.001, and ####P < 0.0001, *Nptxr* siRNA *vs NC* group. ns, not significant. Two-way ANOVA (E and F) and One-way ANOVA (G and H) followed by Bonferroni's tests. n = 8 mice per group. (I and J) Down-regulation of *Nptx2* (I) and *Nptxr* (J) mRNA in TG after *Nptx2*, *Nptxr* siRNA or *NC* siRNA treatment. ***P < 0.001, *Nptx2* siRNA *vs* NC group. ##P < 0.01, *Nptxr* siRNA *vs NC* group. Student's t-test. n = 4–5 mice per group. *NC*, negative control. (K) Scratching behavior following subcutaneous injection IL-31 together with NPTX2 in cheek skin after *Nptxr* siRNA or *NC* siRNA treatment. **P < 0.01 and ****P < 0.0001, compared to *NC* group. Two-way ANOVA followed by Bonferroni's tests. n = 7 mice per group. Data are presented as means ± SEM.

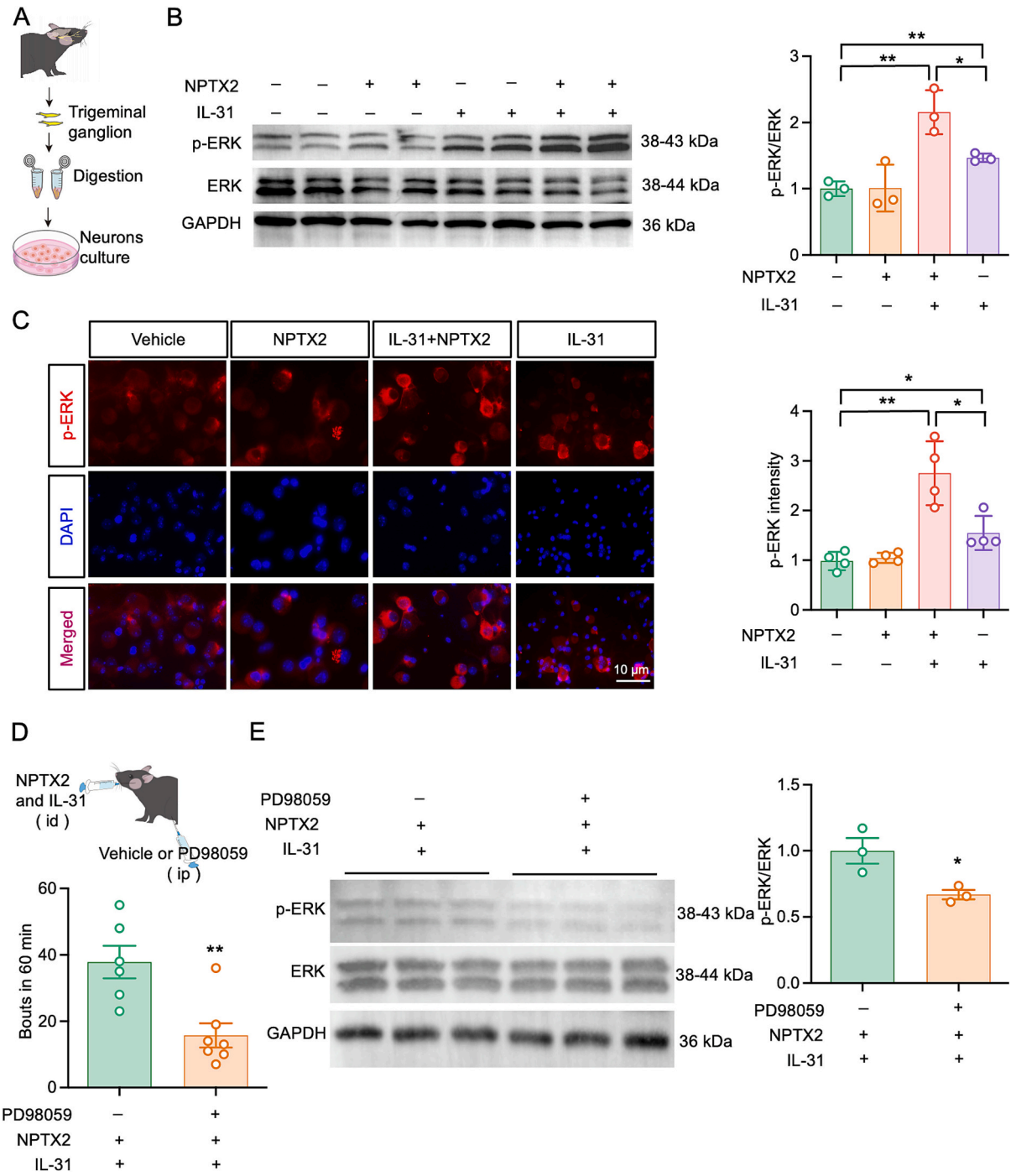

Fig. 6. Neuronal mechanisms of itch involved in NPTX2 combined with IL-31 *in vitro and in vivo*.
(A) Flowchart of TG neuron culture. (B) Bands of p-ERK and ERK (left) in TG neurons 30 min after incubating IL-31 and NPTX2. Statistical chart of the western blot bands (right). *P < 0.05, **P < 0.01. Student's t-test. $n = 3$ mice per group. (C) p-ERK immunostaining (left) in TG neurons after incubating IL-31 and NPTX2. Statistical chart of the immunostaining images (right). *P < 0.05, **P < 0.01. Student's t-test. n = 4 mice per group. Scale bar = 10 μm. (D) Scratching numbers following subcutaneous injection of IL-31 and NPTX2 mixtures in cheek skin pretreated with PD98059 (10 μg). **P < 0.01, compared to the corresponding IL-31 and NPTX2 mixtures group. Student's t-test. n = 7 mice per group. (E) Bands of p-ERK, ERK, and GAPDH expression in TG 30 min after subcutaneous injection of IL-31 and NPTX2 mixtures in cheek skin pretreated with PD98059 (10 μg). Statistical chart of the western blot bands (right). *P < 0.05, compared to the corresponding IL-31 and NPTX2 mixtures. Student's t-test. n = 3 mice per group. Data are presented as means ± SEM.

(Fig. 10).

Our findings, consistent with prior reports [34,56], position neuronal NPTX2 as a pivotal modulator within the peripheral sensory circuitry during chronic itch. The sustained upregulation of NPTX2 in the TG throughout the MC903-induced AD model underscores its role beyond a mere correlative marker. The observed temporal dissociation, where NPTX2 levels continued to rise or remained elevated even as scratching behavior slightly declined from its peak, suggests that NPTX2 may be less critical for the initiation of acute itch episodes and more fundamental to the maintenance of chronic itch. This is further supported by evidence that physical intervention (toenail trimming), which interrupts the itch-scratch cycle, concurrently ameliorates scratching and reduces

Table 1
Docking Score of IL-31R and NPTXR docking.

Model	iptm	ptm
Model0	0.25	0.42
Model1	0.25	0.42
Model2	0.25	0.41
Model3	0.23	0.42
Model4	0.17	0.41

Table 2
Docking Score of OSMR and NPTXR docking.

Model	iptm	ptm
Model0	0.25	0.42
Model1	0.25	0.42
Model2	0.25	0.41
Model3	0.23	0.42
Model4	0.17	0.41

NPTX2 expression [56], indicating that NPTX2 functions as a molecular driver of the self-perpetuating pathology of chronic itch. Its predominant localization within $CGRP^+$ peptidergic neurons, which mediate neurogenic inflammation and pruriceptive transmission *via* neuropeptide release, further supports this role [57,58]. The elongation of $CGRP^+$ afferents into lesioned skin is a recognized pathway for itch persistence [59], and our data suggest that NPTX2 upregulation within this population potentiates this pathway, amplifying pruritic signaling and associated neuroinflammatory responses. Our finding that NPTX2 also localizes to $IB4^+$ non-peptidergic neurons implicates its role in a complementary itch-processing pathway. Historically, research on non-peptidergic neurons has focused on their roles in pain [60], yet emerging evidence underscores their indispensable contribution to itch, particularly in chronic states. Notably, a pivotal study demonstrated that ablation of spinal neurons receiving input from $IB4^+$ afferents profoundly suppresses chronic itch while leaving acute itch largely intact, positioning this circuit as a critical gateway for itch chronicity [61]. $IB4^+$ neurons exhibit heightened excitability and contribute to scratching behaviors in a dry skin model of chronic itch, demonstrating their plasticity and maladaptive role under disease conditions [62]. However, the mere presence of a ligand within a neuronal population is insufficient to define a functional circuit; the requisite expression of its cognate receptor confers signaling specificity and capacity. The predominant localization of NPTXR in pruriceptive $CGRP^+$ and $IB4^+$ neurons further delineates its functional domain within the itch-specific circuitry. Collectively, this specific expression profile solidifies the premise that NPTX2 operates at the core of the peripheral itch network, highlighting it as a compelling and precise therapeutic target for interrupting chronic itch.

Our functional investigations decisively position NPTX2 not as a solitary pruritogen, but as a critical "signal amplifier" within specific peripheral itch pathways. The observation that recombinant NPTX2 alone failed to induce significant scratching behavior, yet potently synergized with IL-31, reveals a fundamental principle of its action: its pruritogenic potency is context-dependent, requiring concurrent activation of a primary cytokine signal. This paradigm provides a mechanistic explanation for the clinical limitations of anti-HIS therapy in AD [63,64], as our data suggest the NPTX2 axis operates predominantly HIS-independent pathways, a notion further supported by the unaltered itch response in NPTX2 knockout mice to histaminergic stimuli [56].

The profound attenuation of chronic itch following intra-TG *Nptx2* or *Nptxr* siRNA knockdown establishes the functional necessity of this ligand-receptor pair within the sensory ganglion for sustaining pathological itch [47,65]. While intra-TG *Nptx2* or *Nptxr* siRNA significantly reduced scratching, it did not rescue MC903-induced weight loss, indicating that the NPTX2-dependent signaling axis is specifically involved in pruritus modulation. The observed weight loss is likely attributable to other aspects of disease pathology, as the energetic cost of sustained inflammation and barrier repair can contribute to negative energy balance [66].

Most compellingly, disruption of the NPTX2-IL-31 synergy by *Nptxr* siRNA provides direct mechanistic insight, demonstrating that the NPTX2/NPTXR complex functions as a privileged signaling module that actively intercepts and amplifies the IL-31 cascade within peripheral neurons. More importantly, the observed potentiation of IL-31-evoked itch by NPTX2 is characterized by distinct temporal kinetics, revealing a critical mechanistic nuance. While the initial 1-h response is consistent with an additive effect, a robust and sustained synergistic enhancement emerges specifically during the 3–5 h post-injection window. This process likely involves the anterograde trafficking of NPTX2 to peripheral terminals and the progressive engagement of downstream effectors such as ERK. The incomplete suppression of itch by siRNA is not merely a technical limitation but likely reflects the multifaceted nature of chronic itch, wherein additional pruritogenic mechanisms (*e.g.*, thymic stromal lymphopoietin, IL-4, IL-13) operate alongside the NPTX2-amplified IL-31 pathway [67,68].

Our study has several limitations. First, the transient efficacy of siRNA precludes a definitive assessment of long-term NPTX2 ablation; future studies employing conditional knockout models will be invaluable. Second, although we focused on its peripheral role, particularly at nerve terminals in the skin, NPTX2 is also known to traffic to central terminals in the spinal cord [56]. Nevertheless, our findings unequivocally establish peripheral NPTX2/NPTXR signaling as a potent amplifier of IL-31-driven pruritus, highlighting a novel and therapeutically targetable node within the complex network of chronic itch.

Our data delineate a precise molecular mechanism through which NPTX2 amplifies IL-31-evoked itch: synergistic hyperactivation of the ERK/mitogen-activated protein kinase signaling pathway. Whereas IL-31 alone is sufficient to induce ERK phosphorylation in sensory neurons [22,69] NPTX2 by itself failed to elicit significant ERK phosphorylation. However, co-application of NPTX2 with IL-31 resulted in a markedly enhanced p-ERK response compared to IL-31 stimulation alone. This synergistic effect provides a clear molecular correlate for the observed behavioral synergy and aligns with the established role of ERK as a critical mediator of both acute and chronic itch signaling in the periphery [70,71]. A key question was how the NPTX2/NPTXR complex interfaces with the IL-31 receptor to achieve this synergy. Our molecular docking and Co-IP analyses provide a definitive answer: NPTXR does not directly interact with the IL-31 receptor complex (IL-31RA/OSMRβ). We propose that the NPTX2/NPTXR and IL-31/IL-31RA axes function as parallel, independent input modules that converge primarily at the level of intracellular ERK activation, and potentially other shared downstream effectors, within the same pruriceptive neuron [24].

Central to our findings is the elucidation of a pathogenic positive-feedback loop that drives the transition from acute pruritic challenge to chronic itch sensitization. This self-reinforcing circuit is initiated when key pruritogens, notably IL-31, stimulate TG neurons, triggering the synthesis and release of NPTX2. The critical, newly identified step is the anterograde transport of NPTX2 to peripheral nerve terminals, where it acts locally to dramatically potentiate IL-31-induced ERK hyperactivation. Sensory neurons not only transmit signals but also actively participate in disease pathogenesis by releasing neurotransmitters. This is classically exemplified by unmyelinated C-fibers, which release neuropeptides such as CGRP and Substance P from their peripheral terminals to induce neurogenic inflammation and potentiate itch [47,72,73]. However, NPTX2 represents a distinct class of "modulatory messenger," it does not directly initiate inflammation or itch like a classic neuropeptide, but instead functions as a potent signal amplifier, specifically tuning the gain of the immune-derived cytokine IL-31. Our discovery that both IL-31 and NPTX2 protein levels are synchronously and significantly elevated in lesional skin at days 6 and 10 of the MC903 model provides crucial *in vivo* validation of this feedback loop. This co-

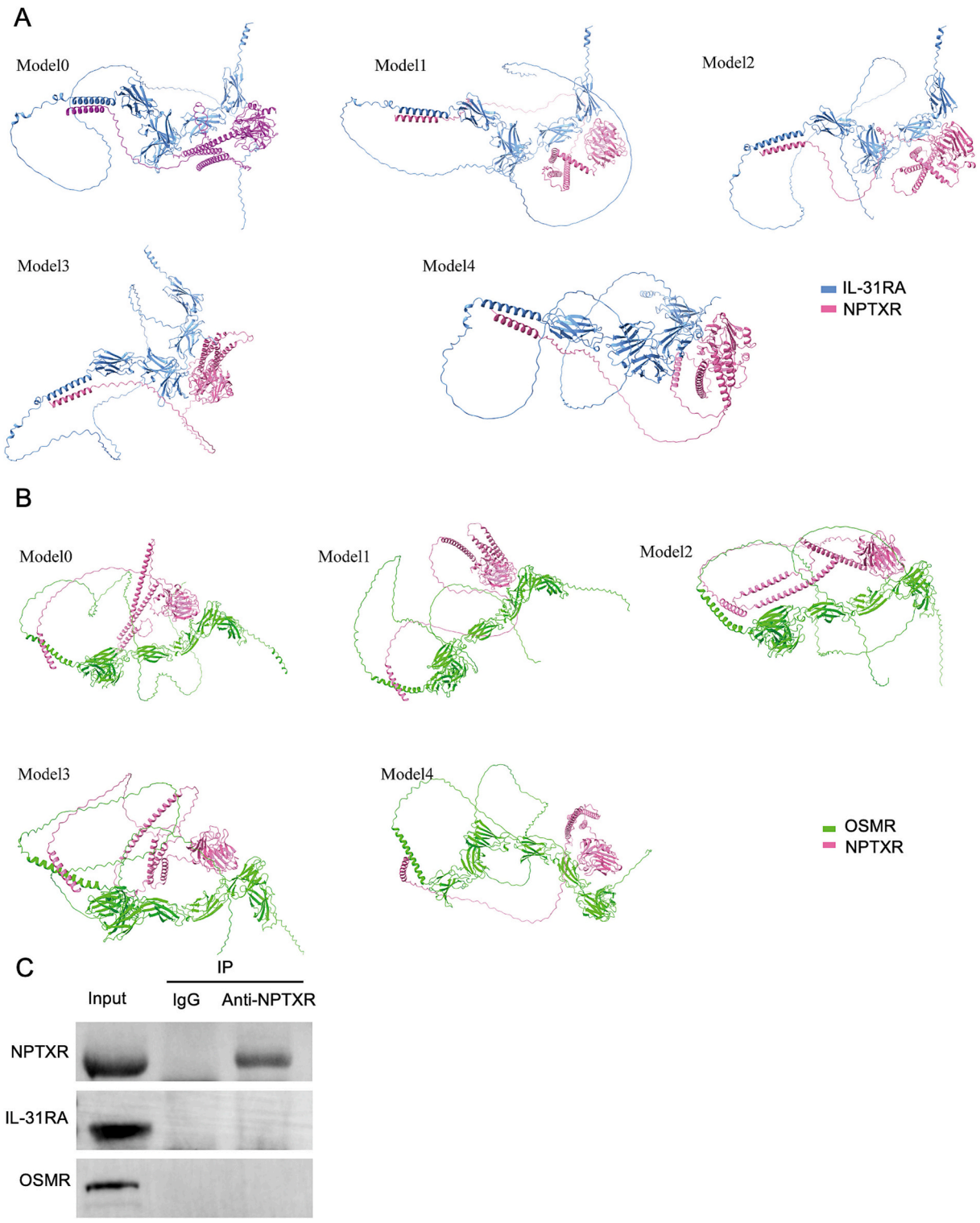

Fig. 7. NPTXR is less likely to interact with IL-31RA and OSMR.
(A) Molecular docking analysis of modeled NPTXR to IL-31RA. (B) Molecular docking analysis of modeled NPTXR to OSMR. (C) Co-IP showing the interaction between NPTXR and IL-31RA/OSMR in skin tissue.

upregulation is not merely correlative; it reflects the active operation of the NPTX2 amplifier circuit within the diseased tissue microenvironment.

The persistent elevation of NPTX2 in both murine and human AD skin, even as itch behavior enters a sustained phase, suggests that NPTX2 plays a fundamental role in maintaining the chronic itch state by establishing a localized, self-perpetuating signaling niche at the interface between sensory nerves and the inflamed skin. Spatially, this loop operates through a dual-axis NPTX2 trafficking pathway: the newly identified anterograde transport to peripheral terminals complements its previously described central transport to the dorsal horn [56]. The discovery of this NPTX2-driven circuit significantly extends the existing neuro-immune axis, revealing a mechanism whereby the nervous system not only responds to immune signals but also deploys its own amplifier

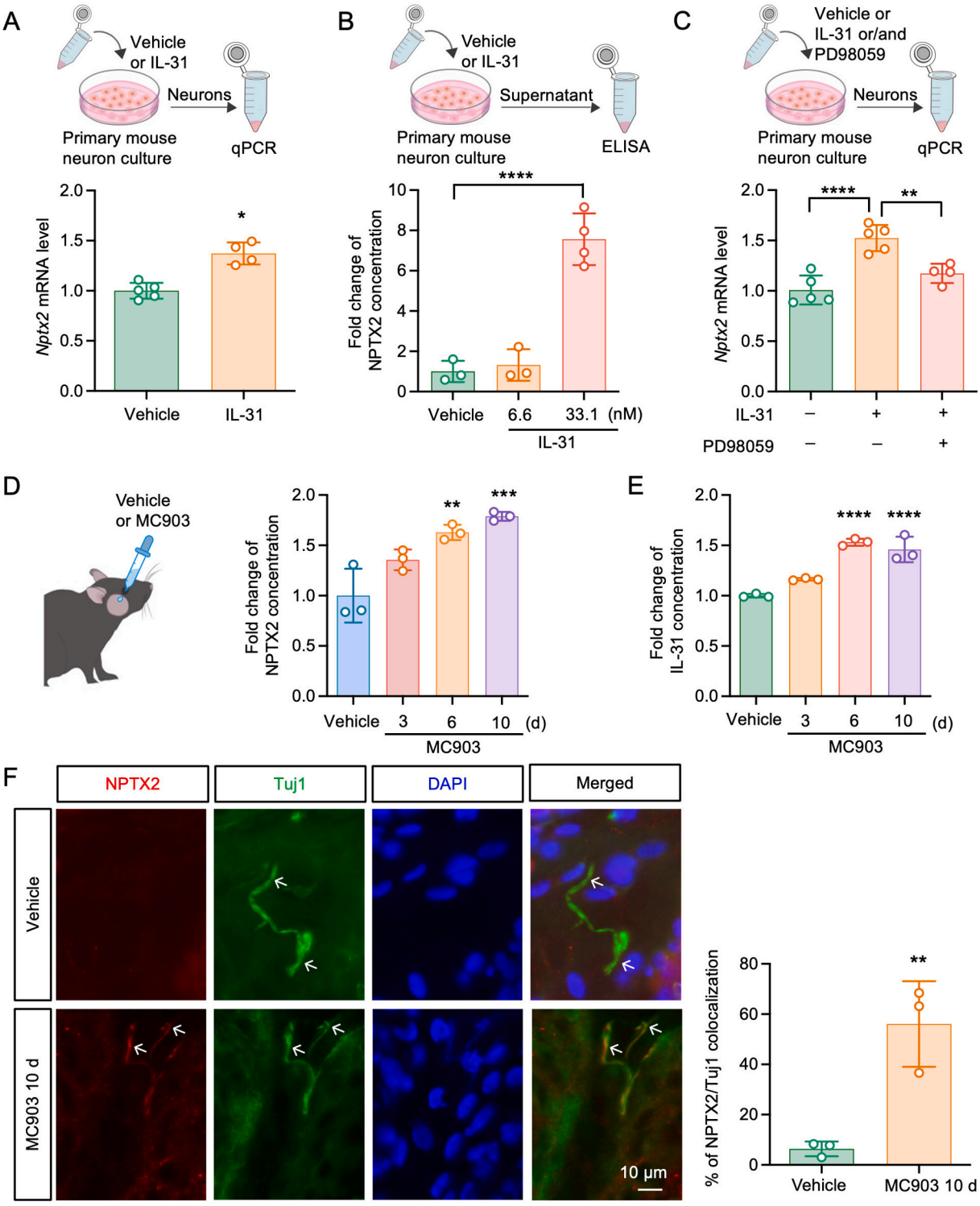

Fig. 8. NPTX2 is synthesized in TG neurons under itchy conditions.
(A) The change of *Nptx2* mRNA level in TG neurons by IL-31-treated. *P < 0.05, compared to vehicle group. Student's t-test. n = 4 to 5 mice per group. (B) Fold change of NPTX2 protein levels in cell supernatant as measured by ELISA 24 h after IL-31-treated at different concentrations. ****P < 0.0001, compared to vehicle group. One-way ANOVA followed by Bonferroni's test. n = 3 to 4 mice per group. (C) qPCR showing *Nptx2* mRNA expression in TG neurons at 6 h after incubating IL-31 alone or combined with PD98059. **P < 0.01, ****P < 0.0001, compared to the IL-31 alone application group. One-way ANOVA followed by Bonferroni's tests. n = 4 to 5 mice per group. (D) ELISA showing NPTX2 protein expression in the skin at 3, 6, 10 days in MC903 mice. **P < 0.01, ***P < 0.001, compared to the vehicle group. One-way ANOVA followed by Bonferroni's tests. n = 3 mice per group. (E) ELISA showing IL-31 protein expression in the skin at 3, 6, 10 days in MC903 mice. ****P < 0.0001, compared to the vehicle group. One-way ANOVA followed by Bonferroni's tests. n = 3 mice per group. (F) Double staining of NPTX2 and Tuj1 (left) in the facial skin at MC903 10 d. Statistical chart (right) of images on the left. **P < 0.01, compared to vehicle group. Scale bar = 10 μm. Student's t-test. n = 3 mice per group. Data are presented as means ± SEM.

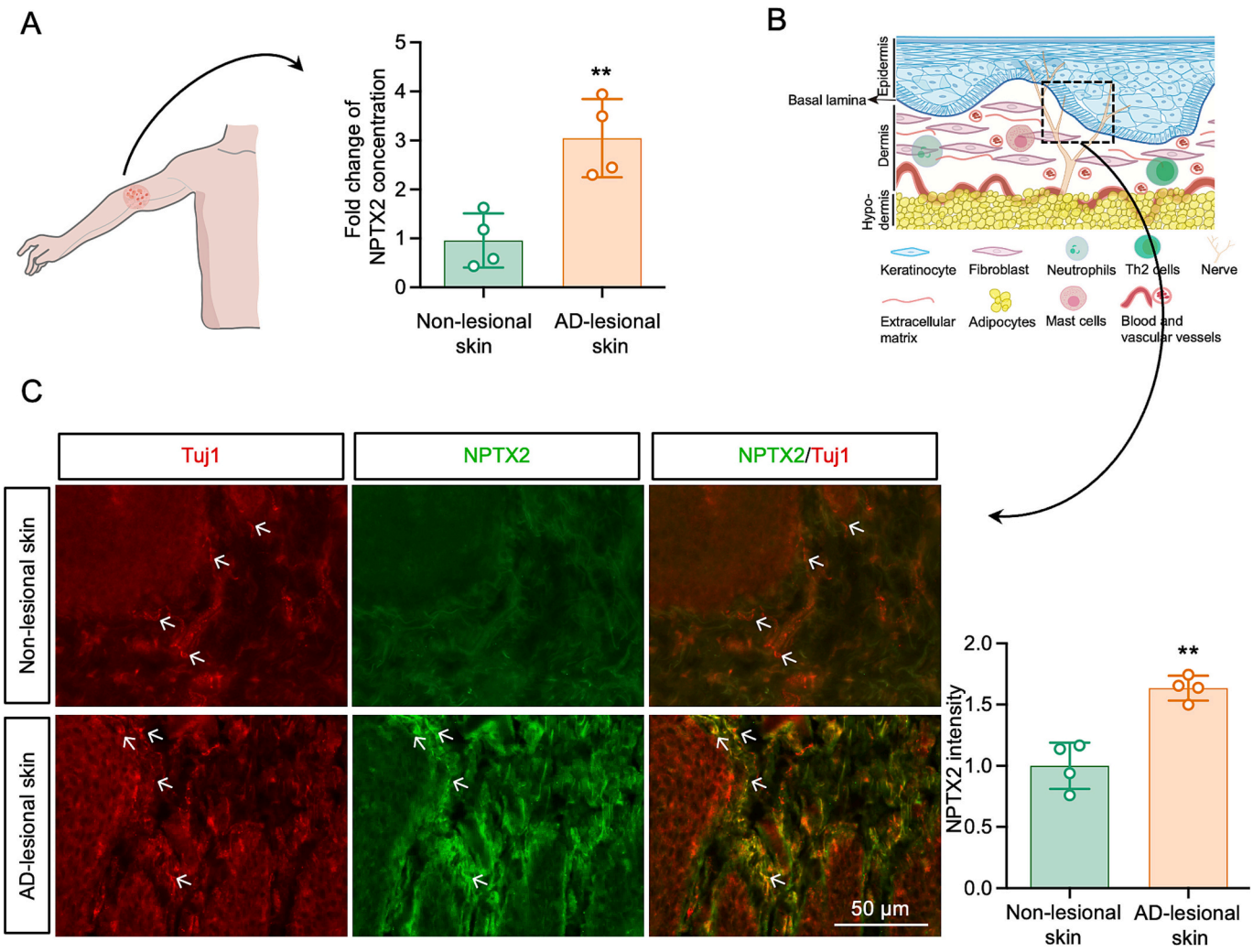

Fig. 9. NPTX2 expression significantly increases in AD patients.
(A) NPTX2 levels measured by ELISA in AD patients. **P < 0.01, compared to non-lesional skin. Student's t-test. n = 4 samples per group. (B) Skin architecture. (C) Representative images showing NPTX2 and Tuj1 (left) in non-lesional and AD-lesional skin of patients. Statistical chart (right) of images (left). **P < 0.01, compared to non-lesional skin. Scale bar = 50 μm. Student's t-test. n = 4 samples per group. Data are presented as means ± SEM.

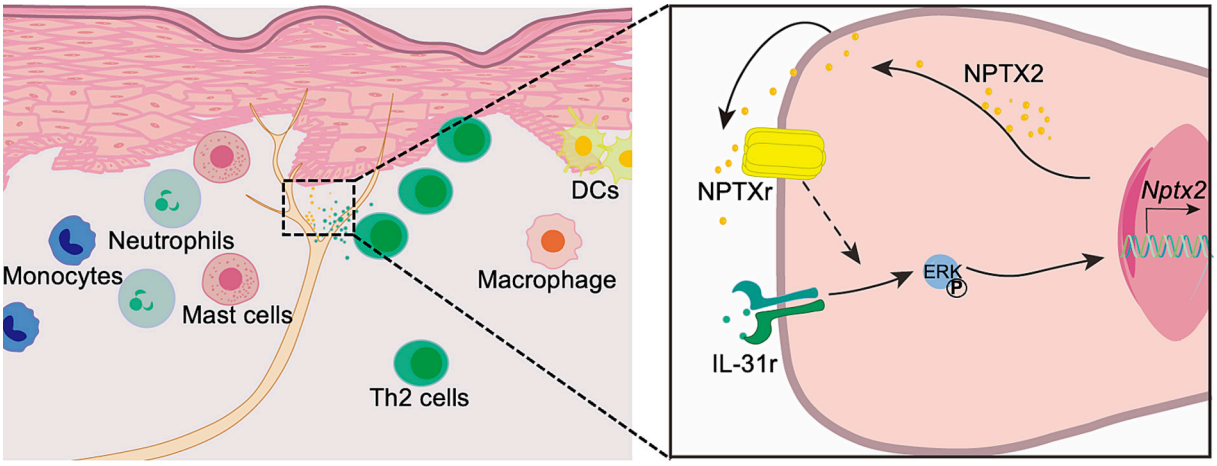

Fig. 10. Working model for NPTX2 contributing to modulation of pruritus in AD.
NPTX2 expression was localized to TG neurons under pruritogenic conditions, and subsequently transported to peripheral nerve terminals, where NPTX2 synergizes with IL-31 by enhancing the phosphorylation of ERK in primary sensory neurons. Created with Adobe Illustrator 2023 and PowerPoint software.

to actively shape and sustain the pathological state, thereby underpinning the intractable nature of chronic itch [74].

In conclusion, this study elucidates the critical role of peripheral sensory neuronal NPTX2 in modulating pruriceptive signaling through both autocrine and paracrine mechanisms. Our experimental findings demonstrate that: (1) MC903-induced cutaneous inflammation significantly upregulates NPTX2 expression in TG neurons; (2) NPTX2 potentiates IL-31-evoked pruritus *via* p-ERK signaling cascades in sensory neurons; and (3) pruritogen-activated neurons exhibit anterograde axonal transport of NPTX2 to peripheral nerve terminals. Collectively, these translational findings establish NPTX2 as a pivotal molecular nexus integrating neuroimmune interactions in both acute and chronic itch pathogenesis, highlighting its potential as a promising therapeutic target for the development of mechanistically distinct antipruritic agents.

CRediT authorship contribution statement

Xue-Qiang Bai: Data curation. **Bing-Xin Wu:** Resources. **Ji-An Wang:** Resources. **Cheng He:** Writing – original draft. **Yong-Liang Shen:** Writing – original draft. **Xiao Wei:** Writing – review & editing. **Yu-Qi Zhang:** Writing – review & editing. **Xue-Wen Chen:** Software. **Rong Sun:** Software. **Qun-Feng Gui:** Conceptualization. **Juan Wang:** Writing – review & editing. **Zhi-Jun Zhang:** Funding acquisition.

Declaration of competing interest

All authors declare that they have no known competing financial interests or personal relationships that could have influenced the work reported in this paper.

Acknowledgments

We are grateful to all the authors for their valuable contributions to this study. This work was supported by the National Natural Science Foundation of China (grants: 82371229 and 31970938). We also acknowledge the use of Adobe Illustrator 2023 and PowerPoint software.

Appendix A. Supplementary data

Supplementary data to this article can be found online at https://doi.org/10.1016/j.intimp.2026.116223.

Data availability

Data will be made available on request.

References

[1] S. de Lusignan, H. Alexander, C. Broderick, J. Dennis, A. McGovern, C. Feeney, C. Flohr, The epidemiology of eczema in children and adults in England: a population-based study using primary care data, Clin. Exp. Allergy 51 (3) (2021) 471–482.
[2] K.M. Sanders, T. Akiyama, The vicious cycle of itch and anxiety, Neurosci. Biobehav. Rev. 87 (2018) 17–26.
[3] M.R. Mack, B.S. Kim, The itch-scratch cycle: a Neuroimmune perspective, Trends Immunol. 39 (12) (2018) 980–991.
[4] M. Tominaga, K. Takamori, Peripheral itch sensitization in atopic dermatitis, Allergol. Int. 71 (3) (2022) 265–277.
[5] S. Gkalpakiotis, S. Kannenberg, K. Kingo, H.R. Nada, M.R. Rakhmatulina, A. Lesiak, A.C. Nicolescu, R. Darlenski, A. Masri, L. Zhou, T. Albuquerque, S. Hammad, I. Almasry, Real-world clinical, psychosocial, and economic burden of atopic dermatitis: results from the ESSENTIAL AD multicountry study, Dermatol. Ther. (Heidelb.) 14 (5) (2024) 1173–1187.
[6] T. Xiao, M. Sun, C. Zhao, J. Kang, TRPV1: a promising therapeutic target for skin aging and inflammatory skin diseases, Front. Pharmacol. 14 (2023) 1037925.
[7] F. Breviario, E.M. d'Aniello, J. Golay, G. Peri, B. Bottazzi, A. Bairoch, S. Saccone, R. Marzella, V. Predazzi, M. Rocchi, et al., Interleukin-1-inducible genes in endothelial cells. Cloning of a new gene related to C-reactive protein and serum amyloid P component, J. Biol. Chem. 267 (31) (1992) 22190–22197.
[8] B. Bottazzi, C. Garlanda, G. Salvatori, P. Jeannin, A. Manfredi, A. Mantovani, Pentraxins as a key component of innate immunity, Curr. Opin. Immunol. 18 (1) (2006) 10–15.
[9] R.J. O'Brien, D. Xu, R.S. Petralia, O. Steward, R.L. Huganir, P. Worley, Synaptic clustering of AMPA receptors by the extracellular immediate-early gene product Narp, Neuron 23 (2) (1999) 309–323.
[10] D.C. Dodds, I.A. Omeis, S.J. Cushman, J.A. Helms, M.S. Perin, Neuronal pentraxin receptor, a novel putative integral membrane pentraxin that interacts with neuronal pentraxin 1 and 2 and taipoxin-associated calcium-binding protein 49, J. Biol. Chem. 272 (34) (1997) 21488–21494.
[11] S.W. Han, Y.H. Park, P.J. Bice, D.A. Bennett, S. Kim, A.J. Saykin, K. Nho, miR-133b as a potential regulator of a synaptic NPTX2 protein in Alzheimer's disease, Ann. Clin. Transl. Neurol. 11 (10) (2024) 2799–2804.
[12] M. Hruska-Plochan, V.I. Wiersma, K.M. Betz, I. Mallona, S. Ronchi, Z. Maniecka, E. M. Hock, E. Tantardini, F. Laferriere, S. Sahadevan, V. Hoop, I. Delvendahl, M. Perez-Berlanga, B. Gatta, M. Panatta, A. van der Bourg, D. Bohaciakova, P. Sharma, L. De Vos, K. Frontzek, A. Aguzzi, T. Lashley, M.D. Robinson, T. Karayannis, M. Mueller, A. Hierlemann, M. Polymenidou, A model of human neural networks reveals NPTX2 pathology in ALS and FTLD, Nature 626 (8001) (2024) 1073–1083.
[13] T. Kang, C. Zhang, H. Lei, R. Luo, M. Liu, S. Wang, X. Zhang, Q. Duan, S. Xiao, Y. Zheng, NPTX2 promotes epithelial-mesenchymal transition in cutaneous squamous cell carcinoma through METTL3-mediated N6-Methyladenosine methylation of SNAIL, J. Invest. Dermatol. 143 (6) (2023) 977–988 e2.
[14] X. Han, Y. Lu, X. Li, L. Xia, H. Wen, Z. Feng, X. Ju, X. Chen, X. Wu, Overexpression of NPTX2 promotes malignant phenotype of epithelial ovarian carcinoma via IL6-JAK2/STAT3 signaling pathway under hypoxia, Front. Oncol. 11 (2021) 643986.
[15] C. Xu, G. Tian, C. Jiang, H. Xue, M. Kuerbanjiang, L. Sun, L. Gu, H. Zhou, Y. Liu, Z. Zhang, Q. Xu, NPTX2 promotes colorectal cancer growth and liver metastasis by the activation of the canonical Wnt/beta-catenin pathway via FZD6, Cell Death Dis. 10 (3) (2019) 217.
[16] Z. Wang, T. Jin, Q. Le, C. Liu, X. Wang, F. Wang, L. Ma, Retrieval-driven hippocampal NPTX2 plasticity facilitates the extinction of cocaine-associated context memory, Biol. Psychiatry 87 (11) (2020) 979–991.
[17] M. Miskimon, S. Han, J.J. Lee, M. Ringkamp, M.A. Wilson, R.S. Petralia, X. Dong, P.F. Worley, J.M. Baraban, I.M. Reti, Selective expression of Narp in primary nociceptive neurons: role in microglia/macrophage activation following nerve injury, J. Neuroimmunol. 274 (1–2) (2014) 86–95.
[18] T. Yan, R. Wang, J. Yao, M. Luo, Single-cell transcriptomic analysis reveals rich pituitary-immune interactions under systemic inflammation, PLoS Biol. 21 (12) (2023) e3002403.
[19] A. Swanson, A.A. Willette, I., Alzheimer's disease neuroimaging, neuronal Pentraxin 2 predicts medial temporal atrophy and memory decline across the Alzheimer's disease spectrum, Brain Behav. Immun. 58 (2016) 201–208.
[20] S.R. Dillon, C. Sprecher, A. Hammond, J. Bilsborough, M. Rosenfeld-Franklin, S. R. Presnell, H.S. Haugen, M. Maurer, B. Harder, J. Johnston, S. Bort, S. Mudri, J. L. Kuijper, T. Bukowski, P. Shea, D.L. Dong, M. Dasovich, F.J. Grant, L. Lockwood, S.D. Levin, C. LeCiel, K. Waggie, H. Day, S. Topouzis, J. Kramer, R. Kuestner, Z. Chen, D. Foster, J. Parrish-Novak, J.A. Gross, Interleukin 31, a cytokine produced by activated T cells, induces dermatitis in mice, Nat. Immunol. 5 (7) (2004) 752–760.
[21] C. Nakashima, A. Otsuka, K. Kabashima, Interleukin-31 and interleukin-31 receptor: new therapeutic targets for atopic dermatitis, Exp. Dermatol. 27 (4) (2018) 327–331.
[22] I.S. Bagci, T. Ruzicka, IL-31: a new key player in dermatology and beyond, J. Allergy Clin. Immunol. 141 (3) (2018) 858–866.
[23] K. Swierczynska, P.K. Krajewski, D. Nowicka-Suszko, R. Bialynicki-Birula, M. Krajewska, J.C. Szepietowski, The serum level of IL-31 in patients with chronic kidney disease-associated pruritus: what can we expect? Toxins (Basel) 14 (3) (2022) 193.
[24] F. Cevikbas, X. Wang, T. Akiyama, C. Kempkes, T. Savinko, A. Antal, G. Kukova, T. Buhl, A. Ikoma, J. Buddenkotte, V. Soumelis, M. Feld, H. Alenius, S.R. Dillon, E. Carstens, B. Homey, A. Basbaum, M. Steinhoff, A sensory neuron-expressed IL-31 receptor mediates T helper cell-dependent itch: involvement of TRPV1 and TRPA1, J. Allergy Clin. Immunol. 133 (2) (2014) 448–460.
[25] U. Raap, M. Gehring, S. Kleiner, U. Rudrich, B. Eiz-Vesper, H. Haas, A. Kapp, B. F. Gibbs, Human basophils are a source of - and are differentially activated by - IL-31, Clin. Exp. Allergy 47 (4) (2017) 499–508.
[26] A. Kato, E. Fujii, T. Watanabe, Y. Takashima, H. Matsushita, T. Furuhashi, A. Morita, Distribution of IL-31 and its receptor expressing cells in skin of atopic dermatitis, J. Dermatol. Sci. 74 (3) (2014) 229–235.
[27] S. Lee, N.Y. Lim, M.S. Kang, Y. Jeong, J.O. Ahn, J.H. Choi, J.Y. Chung, IL-31RA and TRPV1 expression in atopic dermatitis induced with Trinitrochlorobenzene in Nc/Nga mice, Int. J. Mol. Sci. 24 (17) (2023) 13521.
[28] I. Arai, S. Saito, Interleukin-31 receptor a expression in the dorsal root ganglion of mice with atopic dermatitis, Int. J. Mol. Sci. 24 (2) (2023) 1047.
[29] A. Ruppenstein, M.M. Limberg, K. Loser, A.E. Kremer, B. Homey, U. Raap, Involvement of neuro-immune interactions in pruritus with special focus on receptor expressions, Front Med (Lausanne) 8 (2021) 627985.
[30] C. Cornelissen, J. Luscher-Firzlaff, J.M. Baron, B. Luscher, Signaling by IL-31 and functional consequences, Eur. J. Cell Biol. 91 (6–7) (2012) 552–566.
[31] Z.Q. Zhao, F.Q. Huo, J. Jeffry, L. Hampton, S. Demehri, S. Kim, X.Y. Liu, D. M. Barry, L. Wan, Z.C. Liu, H. Li, A. Turkoz, K. Ma, L.A. Cornelius, R. Kopan, J. F. Battey Jr., J. Zhong, Z.F. Chen, Chronic itch development in sensory neurons requires BRAF signaling pathways, J. Clin. Invest. 123 (11) (2013) 4769–4780.

[32] X. Liu, Y. Wang, T. Tao, L. Zeng, D. Wang, Y. Wen, Y. Li, Z. Zhao, A. Tao, GRPR/extracellular signal-regulated kinase and NPRA/extracellular signal-regulated kinase signaling pathways play a critical role in spinal transmission of chronic itch, J. Invest. Dermatol. 141 (4) (2021) 863–873.
[33] Y. Hirata, H. Brems, S. Van der Auweraer, M. Ohyagi, M. Iizuka, S. Mise-Omata, M. Ito, L. Messiaen, S. Mizuno, S. Takahashi, E. Legius, A. Yoshimura, Legius syndrome mutations in the Ras-regulator SPRED1 abolish its membrane localization and potentially cause neurodegeneration, J. Biol. Chem. 300 (12) (2024) 107969.
[34] C.M. Walsh, R.Z. Hill, J. Schwendinger-Schreck, J. Deguine, E.C. Brock, N. Kucirek, Z. Rifi, J. Wei, K. Gronert, R.B. Brem, G.M. Barton, D.M. Bautista, Neutrophils promote CXCR3-dependent itch in the development of atopic dermatitis, Elife 8 (2019) e48448.
[35] Q. Zhang, M.D. Zhu, D.L. Cao, X.Q. Bai, Y.J. Gao, X.B. Wu, Chemokine CXCL13 activates p38 MAPK in the trigeminal ganglion after infraorbital nerve injury, Inflammation 40 (3) (2017) 762–769.
[36] Q. Zhang, D.L. Cao, Z.J. Zhang, B.C. Jiang, Y.J. Gao, Chemokine CXCL13 mediates orofacial neuropathic pain via CXCR5/ERK pathway in the trigeminal ganglion of mice, J. Neuroinflammation 13 (1) (2016) 183.
[37] Z.J. Zhang, H.Y. Shao, C. Liu, H.L. Song, X.B. Wu, D.L. Cao, M. Zhu, Y.Y. Fu, J. Wang, Y.J. Gao, Descending dopaminergic pathway facilitates itch signal processing via activating spinal GRPR(+) neurons, EMBO Rep. 24 (10) (2023) e56098.
[38] Y. Xu, Y. Qu, C. Zhang, C. Niu, X. Tang, X. Sun, K. Wang, Selective inhibition of overactive warmth-sensitive ca(2+)-permeable TRPV3 channels by antispasmodic agent flopropione for alleviation of skin inflammation, J. Biol. Chem. 300 (2) (2024) 105595.
[39] J.I. Silverberg, A. Wollenberg, A. Reich, D. Thaci, F.J. Legat, K.A. Papp, L. Stein Gold, J.D. Bouaziz, A.E. Pink, J.M. Carrascosa, B. Rewerska, J. C. Szepietowski, D. Krasowska, B. Havlickova, M. Kalowska, N. Magnolo, S. Pauser, N. Nami, M.B. Sauder, V. Jain, K. Padlewska, S.Y. Cheong, P. Fleuranceau Morel, L. Ulianov, C. Piketty, A.S. Arcadia, Investigators, Nemolizumab with concomitant topical therapy in adolescents and adults with moderate-to-severe atopic dermatitis (ARCADIA 1 and ARCADIA 2): results from two replicate, double-blind, randomised controlled phase 3 trials, Lancet 404 (10451) (2024) 445–460.
[40] H. Wiegmann, L. Renkhold, C. Zeidler, K. Agelopoulos, S. Stander, Interleukin profiling in atopic dermatitis and chronic nodular Prurigo, Int. J. Mol. Sci. 25 (15) (2024) 8445.
[41] N. Yang, J. Deng, H. Xu, H. Dai, H. Jin, H. Shao, Y. Liu, Anti-atopic dermatitis effect of fraxinellone via inhibiting IL-31 in vivo and in vitro, Heliyon 10 (15) (2024) e35391.
[42] A. Ikoma, R. Rukwied, S. Stander, M. Steinhoff, Y. Miyachi, M. Schmelz, Neuronal sensitization for histamine-induced itch in lesional skin of patients with atopic dermatitis, Arch. Dermatol. 139 (11) (2003) 1455–1458.
[43] J. Xu, C. Pittenger, The histamine H3 receptor modulates dopamine D2 receptor-dependent signaling pathways and mouse behaviors, J. Biol. Chem. 299 (4) (2023) 104583.
[44] X. Dong, X. Dong, Peripheral and central mechanisms of itch, Neuron 98 (3) (2018) 482–494.
[45] F. Wang, B.S. Kim, Itch: a paradigm of Neuroimmune crosstalk, Immunity 52 (5) (2020) 753–766.
[46] M.S. Fassett, J.M. Braz, C.A. Castellanos, J.J. Salvatierra, M. Sadeghi, X. Yu, A. W. Schroeder, J. Caston, P. Munoz-Sandoval, S. Roy, S. Lazarevsky, D.J. Mar, C. J. Zhou, J.S. Shin, A.I. Basbaum, K.M. Ansel, IL-31-dependent neurogenic inflammation restrains cutaneous type 2 immune response in allergic dermatitis, Sci Immunol 8 (88) (2023) eabi6887.
[47] Q. Liu, Z. Tang, L. Surdenikova, S. Kim, K.N. Patel, A. Kim, F. Ru, Y. Guan, H. J. Weng, Y. Geng, B.J. Undem, M. Kollarik, Z.F. Chen, D.J. Anderson, X. Dong, Sensory neuron-specific GPCR Mrgprs are itch receptors mediating chloroquine-induced pruritus, Cell 139 (7) (2009) 1353–1365.
[48] S. Takahashi, S. Ochiai, J. Jin, N. Takahashi, S. Toshima, H. Ishigame, K. Kabashima, M. Kubo, M. Nakayama, K. Shiroguchi, T. Okada, Sensory neuronal STAT3 is critical for IL-31 receptor expression and inflammatory itch, Cell Rep. 42 (12) (2023) 113433.
[49] D.L. Cao, L.J. Ma, B.C. Jiang, Q. Gu, Y.J. Gao, Cytochrome P450 26A1 contributes to the maintenance of neuropathic pain, Neurosci. Bull. 40 (3) (2024) 293–309.
[50] B.C. Jiang, Y.J. Ling, M.L. Xu, J. Gu, X.B. Wu, W.L. Sha, T. Tian, X.H. Bai, N. Li, C. Y. Jiang, O. Chen, L.J. Ma, Z.J. Zhang, Y.B. Qin, M. Zhu, H.J. Yuan, L.J. Wu, R.R. Ji, Y.J. Gao, Follistatin drives neuropathic pain in mice through IGF1R signaling in nociceptive neurons, Sci. Transl. Med. 16 (769) (2024) eadi1564.
[51] G. Wang, M.D.M. Joel, J. Yuan, J. Wang, X. Cai, D.K.W. Ocansey, Y. Yan, H. Qian, X. Zhang, W. Xu, F. Mao, Human umbilical cord mesenchymal stem cells alleviate inflammatory bowel disease by inhibiting ERK phosphorylation in neutrophils, Inflammopharmacology 28 (2) (2020) 603–616.
[52] Y. Liang, Y. Qian, J. Tang, C. Yao, S. Yu, J. Qu, H. Wei, G. Chen, Y. Han, Arsenic trioxide promotes ERK1/2-mediated phosphorylation and degradation of BIM(EL) to attenuate apoptosis in BEAS-2B cells, Chem. Biol. Interact. 369 (2023) 110304.
[53] Y. Liu, J. Tang, J. Yuan, C. Yao, K. Hosoi, Y. Han, S. Yu, H. Wei, G. Chen, Arsenite-induced downregulation of occludin in mouse lungs and BEAS-2B cells via the ROS/ERK/ELK1/MLCK and ROS/p38 MAPK signaling pathways, Toxicol. Lett. 332 (2020) 146–154.
[54] S.Z. Sun, H. Cao, N. Yao, L.L. Zhao, X.F. Zhu, E.A. Ni, Q. Zhu, W.Z. Zhu, B-Arrestin 2 mediates arginine vasopressin-induced IL-6 induction via the ERK(1/2)-NF-κB signal pathway in murine hearts, Acta Pharmacol. Sin. 41 (2) (2020) 198–207.
[55] S.C. Prinster, C. Hague, R.A. Hall, Heterodimerization of g protein-coupled receptors: specificity and functional significance, Pharmacol. Rev. 57 (3) (2005) 289–298.
[56] K. Kanehisa, K. Koga, S. Maejima, Y. Shiraishi, K. Asai, M. Shiratori-Hayashi, M. F. Xiao, H. Sakamoto, P.F. Worley, M. Tsuda, Neuronal pentraxin 2 is required for facilitating excitatory synaptic inputs onto spinal neurons involved in pruriceptive transmission in a model of chronic itch, Nat. Commun. 13 (1) (2022) 2367.
[57] P. Schmidt, U. Pfeil, M. Lafee, S. Petersen, A. Perniss, M. Keshavarz, D. Das, A. Wyatt, U. Boehm, B. Schutz, W. Kummer, K. Deckmann, Tuft cells trigger neurogenic inflammation in the urethra, Cell Rep. 44 (10) (2025) 116370.
[58] V. Bhatia, V. Vikram, A. Rattan, A. Chandel, M.S. Ashawat, Neuroinflammatory crosstalk in migraine: consolidated activity of rizatriptan and meloxicam in suppressing CGRP-induced nociception and COX-mediated inflammation, Inflammopharmacology 33 (7) (2025) 3871–3883.
[59] E.S. McCoy, B. Taylor-Blake, S.E. Street, A.L. Pribisko, J. Zheng, M.J. Zylka, Peptidergic CGRPalpha primary sensory neurons encode heat and itch and tonically suppress sensitivity to cold, Neuron 78 (1) (2013) 138–151.
[60] W.D. Snider, S.B. McMahon, Tackling pain at the source: new ideas about nociceptors, Neuron 20 (4) (1998) 629–632.
[61] S. Sun, Q. Xu, C. Guo, Y. Guan, Q. Liu, X. Dong, Leaky gate model: intensity-dependent coding of pain and itch in the spinal cord, Neuron 93 (4) (2017) 840–853 e5.
[62] T. Akiyama, M. Tominaga, K. Takamori, M.I. Carstens, E. Carstens, Role of spinal bombesin-responsive neurons in nonhistaminergic itch, J. Neurophysiol. 112 (9) (2014) 2283–2289.
[63] L.A. Beck, D. Thaci, J.D. Hamilton, N.M. Graham, T. Bieber, R. Rocklin, J.E. Ming, H. Ren, R. Kao, E. Simpson, M. Ardeleanu, S.P. Weinstein, G. Pirozzi, E. Guttman-Yassky, M. Suarez-Farinas, M.D. Hager, N. Stahl, G.D. Yancopoulos, A.R. Radin, Dupilumab treatment in adults with moderate-to-severe atopic dermatitis, N. Engl. J. Med. 371 (2) (2014) 130–139.
[64] P.A. Klein, R.A. Clark, An evidence-based review of the efficacy of antihistamines in relieving pruritus in atopic dermatitis, Arch. Dermatol. 135 (12) (1999) 1522–1525.
[65] Y.G. Sun, Z.F. Chen, A gastrin-releasing peptide receptor mediates the itch sensation in the spinal cord, Nature 448 (7154) (2007) 700–703.
[66] T. Werfel, J.P. Allam, T. Biedermann, K. Eyerich, S. Gilles, E. Guttman-Yassky, W. Hoetzenecker, E. Knol, H.U. Simon, A. Wollenberg, T. Bieber, R. Lauener, P. Schmid-Grendelmeier, C. Traidl-Hoffmann, C.A. Akdis, Cellular and molecular immunologic mechanisms in patients with atopic dermatitis, J. Allergy Clin. Immunol. 138 (2) (2016) 336–349.
[67] Y. Dong, M.K. Sarkar, Y. Wu, X. Xing, M.T. Patrick, B. Duan, M. Gharaee-Kermani, V. Julia, S. Weidinger, J.M. Kahlenberg, J.E. Gudjonsson, L.C. Tsoi, Endothelin-2 from keratinocytes and its association with itch in skin diseases, J. Invest. Dermatol. (2025).
[68] J. Romantowski, K. Fabianczyk, M. Skrzypkowska, W.J. Cubala, P. Trzonkowski, M. Niedoszytko, IL-4, TSLP and IL-31 cytokine profiles as related to psychometric measures in patients with Mastocytosis, Int. J. Mol. Sci. 26 (2) (2025).
[69] D.N. Che, B.O. Cho, J.S. Kim, J.Y. Shin, H.J. Kang, S.I. Jang, Effect of Luteolin and Apigenin on the production of Il-31 and Il-33 in lipopolysaccharides-activated microglia cells and their mechanism of action, Nutrients 12 (3) (2020).
[70] T.T. Wang, Z.Y. Li, D.D. Hu, X.Y. Xu, N.J. Song, G.Q. Li, L. Zhang, Spinal histamine H4 receptor mediates chronic pruritus via p-ERK in acetone-ether-water (AEW)-induced dry skin mice, Exp. Dermatol. 33 (7) (2024) e15128.
[71] N. Zeze, M. Kido-Nakahara, G. Tsuji, E. Maehara, Y. Sato, S. Sakai, K. Fujishima, A. Hashimoto-Hachiya, M. Furue, T. Nakahara, Role of ERK pathway in the pathogenesis of atopic dermatitis and its potential as a therapeutic target, Int. J. Mol. Sci. 23 (7) (2022) 3467.
[72] A.F. Russo, Calcitonin gene-related peptide (CGRP): a new target for migraine, Annu. Rev. Pharmacol. Toxicol. 55 (2015) 533–552.
[73] J.Y. Ren, J.X. Song, M.Y. Lu, H. Chen, Cardioprotection by ischemic postconditioning is lost in isolated perfused heart from diabetic rats: involvement of transient receptor potential vanilloid 1, calcitonin gene-related peptide and substance P, Regul. Pept. 169 (1–3) (2011) 49–57.
[74] L. Riol-Blanco, J. Ordovas-Montanes, M. Perro, E. Naval, A. Thiriot, D. Alvarez, S. Paust, J.N. Wood, U.H. von Andrian, Nociceptive sensory neurons drive interleukin-23-mediated psoriasiform skin inflammation, Nature 510 (7503) (2014) 157–161.